Evidence of high N_2 fixation rates in the temperate Northeast Atlantic

Debany Fonseca-Batista[1,2], Xuefeng Li[1,3], Virginie Riou[4], Valérie Michotey[4], Florian Deman[1], François Fripiat[5], Sophie Guasco[4], Natacha Brion[1], Nolwenn Lemaitre[1,6,7], Manon Tonnard[6,8], Morgane Gallinari[6], Hélène Planquette[6], Frédéric Planchon[6], Géraldine Sarthou[6], Marc Elskens[1], Julie LaRoche[2], Lei Chou[3], Frank Dehairs[1]

[1] Analytical, Environmental and Geo-Chemistry, Earth System Sciences Research Group, Vrije Universiteit Brussel, 1050 Brussels, Belgium
[2] Department of Biology, Dalhousie University, Halifax, Nova Scotia, Canada B3H 4R2
[3] Service de Biogéochimie et Modélisation du Système Terre, Université Libre de Bruxelles, 1050 Brussels, Belgium
[4] Aix-Marseille Univ, Université de Toulon, CNRS, IRD, MIO, Marseille, France
[5] Max Planck Institute for Chemistry, Climate Geochemistry Department, 55128 Mainz, Germany
[6] Laboratoire des Sciences de l'Environnement MARin – CNRS UMR 6539 – Institut Universitaire Européen de la Mer, 29280 Plouzané, France
[7] Department of Earth Sciences, Institute of Geochemistry and Petrology, ETH-Zürich, 8092 Zürich, Switzerland
[8] Institute for Marine and Antarctic Studies, University of Tasmania, Hobart, TAS 7001, Australia

Correspondence to: Debany Fonseca P. Batista (dbatista8@hotmail.com)

Abstract. Diazotrophic activity and primary production (PP) were investigated along two transects (Belgica BG2014/14 and GEOVIDE cruises) off the western Iberian Margin and the Bay of Biscay in May 2014. Substantial N_2 fixation activity was observed at 8 of the 10 stations sampled, ranging overall from 81 to 384 µmol N m^{-2} d^{-1} (0.7 to 8.2 nmol N L^{-1} d^{-1}), with two sites close to the Iberian Margin situated between 38.8° N and 40.7° N yielding rates reaching up to 1355 and 1533 µmol N m^{-2} d^{-1}. Primary production was relatively lower along the Iberian Margin with rates ranging from 33 to 59 mmol C m^{-2} d^{-1}, while it increased towards the northwest away from the Peninsula, reaching as high as 135 mmol C m^{-2} d^{-1}. In agreement with the area-averaged Chl *a* satellite data contemporaneous with our study period, our results revealed that post-bloom conditions prevailed at most sites, while at the northwesternmost station the bloom was still ongoing. When converted to carbon uptake using Redfield stoichiometry, N_2 fixation could support 1 to 3% of daily PP in the euphotic layer at most sites, except at the two most active sites where this contribution to daily PP could reach up to 25%. At the two sites where N_2 fixation activity was the highest, the prymnesiophyte-symbiont *Candidatus* Atelocyanobacterium thalassa (UCYN-A) dominated the *nifH* sequence pool, while the remaining recovered sequences belonged to non-cyanobacterial phylotypes. At all the other sites however, the recovered *nifH* sequences were exclusively assigned phylogenetically to non-cyanobacterial phylotypes. The intense N_2 fixation activities recorded at the time of our study were likely promoted by the availability of phytoplankton-derived organic matter produced during the spring bloom, as evidenced by the significant surface particulate organic carbon concentrations. Also, the presence of excess phosphorus signature in surface waters seemed to contribute to sustaining N_2 fixation, particularly at the sites with extreme activities. These results provide a mechanistic understanding of the unexpectedly high N_2 fixation in productive waters of the temperate North Atlantic, and highlight the importance of N_2 fixation for future assessment of global N inventory.

1 Introduction

Dinitrogen (N_2) fixation is the major pathway of nitrogen (N) input to the global ocean and thereby contributes to sustaining oceanic primary productivity (Falkowski, 1997). The conversion by N_2-fixing micro-organisms (diazotrophs) of dissolved N_2 gas into bioavailable nitrogen also contributes to new production in the euphotic layer and as such, to the subsequent sequestration of atmospheric carbon dioxide into the deep ocean (Gruber, 2008). Estimating the overall contribution of N_2 fixation to carbon sequestration in the ocean requires an assessment of the global marine N_2 fixation.

Until recently most studies of N_2 fixation have focused on the tropical and subtropical regions of the global ocean, with few attempts to measure N_2 fixation at higher latitudes, with the exception of enclosed brackish seas (Ohlendieck et al., 2000; Luo et al., 2012; Farnelid et al., 2013). The intense research efforts in the low latitude regions stem for the observable presence of cyanobacterial diazotrophs such as the diatom-diazotroph association (DDA) and the colony-forming filamentous *Trichodesmium* (Capone, 1997; Capone et al., 2005; Foster et al., 2007). *Trichodesmium* in particular, was long considered as the most active diazotroph in the global ocean. It has mostly been reported in tropical and subtropical oligotrophic oceanic waters which are thought to represent the optimal environment for its growth and N_2-fixing activity (Dore et al., 2002; Breitbarth et al., 2007; Montoya et al., 2007; Needoba et al., 2007; Moore et al., 2009; Fernández et al., 2010; Snow et al., 2015). In low latitude regions, warm stratified surface waters depleted in dissolved inorganic nitrogen (DIN), are assumed to give a competitive advantage to diazotrophs over other phytoplankton since only they can draw N from the unlimited dissolved N_2 pool for their biosynthesis. As such, past estimates of global annual N_2 fixation were mainly based on information gathered from tropical and subtropical regions, while higher latitude areas have been poorly explored for diazotrophic activity (Luo et al., 2012).

Studies using genetic approaches targeting the *nifH* gene encoding the nitrogenase enzyme, essential for diazotrophy, have shown the presence of diverse diazotrophs throughout the world's oceans, extending their ecological niche (Farnelid et al., 2011; Cabello et al., 2015; Langlois et al., 2015). Small diazotrophs such as unicellular diazotrophic cyanobacteria (UCYN classified in groups A, B and C) and non-cyanobacterial diazotrophs, mostly heterotrophic bacteria (e.g. Alpha- and Gammaproteobacteria), have been observed over a wide range of depths and latitudes, thereby expanding the potential for diazotrophy to a much broader geographic scale (Langlois et al., 2005, 2008; Krupke et al., 2014; Cabello et al., 2015). The discovery of a methodological bias associated to the commonly used $^{15}N_2$ bubble-addition technique (Mohr et al., 2010) and the presence of an abundant diazotrophic community in high latitude regions actively fixing N_2 (Needoba et al., 2007; Rees et al., 2009; Blais et al., 2012; Mulholland et al., 2012; Shiozaki et al., 2015), indicate that more efforts are needed to better constrain oceanic N_2 fixation and diazotrophic diversity at higher latitudes.

In the Northeast Atlantic, the large input of iron-rich Saharan dust alleviating dissolved iron (dFe) limitation of the nitrogenase activity (Fe being a co-factor of the N_2-fixing enzyme) (Raven, 1988; Howard & Rees, 1996; Mills et al., 2004; Snow et al., 2015) and the upwelling of subsurface waters with low DIN (dissolved inorganic nitrogen) to phosphate ratios, make this region highly favorable for N_2 fixation activity (Deutsch et al., 2007; Moore et al., 2009). In addition, the eastern North Atlantic has been observed to harbour a highly active and particularly diverse diazotrophic community (Langlois et al., 2008; Moore et al., 2009; Großkopf et al., 2012; Ratten et al., 2015; Fonseca-Batista et al., 2017) not only in the tropical and subtropical regions but also in the temperate Iberian region which was reported to be a hotspot for the globally important prymnesiophyte-UCYN-A symbiotic associations (Cabello et al., 2015). Earlier studies in the Iberian open waters investigated diazotrophic activity either under stratified water column conditions of boreal summer and autumn (Moore et al., 2009; Benavides et al., 2011; Snow et

al., 2015; Fonseca-Batista et al., 2017) or during the winter convection period (Rijkenberg et al., 2011; Agawin et al., 2014). Here, we present N_2 fixation rate measurements and the taxonomic affiliation of the diazotrophic community from two consecutive campaigns carried out in the Northeast sector of the Atlantic Ocean in May 2014, during and after the spring bloom.

2 Material and Methods

2.1 Site description and sample collection

Field experiments were conducted during two nearly simultaneous cruises in May 2014. The Belgica BG2014/14 cruise (21–30 May 2014, R/V *Belgica*), investigated the Bay of Biscay and the western Iberian Margin. In parallel, the GEOVIDE expedition in the framework of the international GEOTRACES program (GA01 section, May 16 to June 29 2014, R/V *Pourquoi pas?*) sailed from the Portuguese shelf area towards Greenland and ended in Newfoundland, Canada (http://dx.doi.org/10.17600/14000200). N_2 fixation activities were determined at ten stations within the Iberian Basin, among which four sites were investigated during the GEOVIDE cruise (stations Geo-1, Geo-2, Geo-13 and Geo-21) and six sites during the BG2014/14 cruise (stations Bel-3, Bel-5, Bel-7, Bel-9, Bel-11 and Bel-13; Fig. 1).

All sampling sites were located within the Iberian Basin Portugal Current System (PCS) (Ambar and Fiúza, 1994) which is influenced by highly fluctuating wind stresses (Frouin et al., 1990). The predominant upper layer water mass in this basin is the Eastern North Atlantic Central Water (ENACW), a winter-mode water, which according to Fiúza (1984) consists of two components (see θ/S diagrams in Supporting Information Fig. S1): (i) the lighter, relatively warm (> 14 °C) and salty (salinity > 35.6) ENACWst formed in the subtropical Azores Front region (~35° N) when Azores Mode Water is subducted as a result of strong evaporation and winter cooling; and (ii) the colder and less saline ENACWsp, underlying the ENACWst, formed in the subpolar eastern North Atlantic (north of 43° N) through winter cooling and deep convection (McCartney and Talley, 1982). The spatial distribution of these Central Waters allowed the categorization of the sampling sites into 2 groups: (i) ENACWsp stations north of 43° N (Bel-3, Bel-5, Bel-7, and Geo-21) only affected by the ENACWsp (Fig. S1a, b) and (ii) ENACWst stations, south of 43° N, characterized by an upper layer influenced by the ENACWst and an subsurface layer, by the ENACWsp (Fig. S1a, b). Most of the ENACWst stations were open ocean sites (Bel-9, Bel-11, Bel-13, and Geo-13) while two stations were in proximity of the Iberian shelf (Geo-1 and Geo-2) (Tonnard et al., 2018).

Temperature, salinity and photosynthetically active radiation (PAR) profiles down to 1500 m depth were obtained using a conductivity-temperature-depth (CTD) sensor (SBE 09 and SBE 911+, during the BG2014/14 and GEOVIDE cruises, respectively) fitted to the rosette frames. For all biogeochemical measurements, seawater samples were collected with Niskin bottles attached to the rosette and closed at specific depths in the upper 200 m. In particular, for stable isotope incubation experiments seawater was collected in 4.5 L acid-cleaned polycarbonate (PC) bottles from four depths corresponding to 54%, 13%, 3% and 0.2% of surface PAR at stations Bel-3, Bel-5, Bel-7, Bel-9, Bel-11, and Geo-2. At stations Geo-1, Geo-13 and Geo-21, two additional depths corresponding to 25% and 1% of surface PAR were also sampled for the same purpose.

2.2 Nutrient measurements

Ammonium (NH_4^+) concentrations were measured on board during both cruises, while nitrate + nitrite ($NO_3^- + NO_2^-$) concentrations were measured on board only during the GEOVIDE expedition. During the BG2014/14 cruise,

samples for NO_3^- + NO_2^- and phosphate (PO_4^{3-}) measurements were filtered (0.2 µm) and stored at –20 °C until analysis at the home-based laboratory. PO_4^{3-} data are not available for the GEOVIDE cruise.

Nutrient concentrations were determined using the conventional fluorometric (for NH_4^+) (Holmes et al., 1999) and colorimetric methods (for the other nutrients) (Grasshoff et al., 1983) with detection limits (DL) of 64 nmol L^{-1} (NH_4^+), 90 nmol L^{-1} (NO_3^- + NO_2^-) and 60 nmol L^{-1} (PO_4^{3-}). For the BG2014/14 cruise, chlorophyll *a* (Chl *a*) concentrations were determined according to Yentsch and Menzel (1963). Briefly, 250 mL of seawater was filtered onto Whatman GF/F glass microfiber filters (0.7 µm nominal pore size), followed by pigment extraction in 90% acetone, centrifugation and fluorescence measurement using a Shimadzu RF-150 fluorometer. For the GEOVIDE cruise, Chl *a* concentrations were measured as described in Ras et al. (2008). Briefly, filters samples were extracted in 100% methanol, disrupted by sonification, and clarified by vacuum filtration through Whatman GF/F filters. The extracts were analysed by high-performance liquid chromatography (HPLC Agilent Technologies 1200).

2.3 $^{15}N_2$ fixation and ^{13}C-HCO_3^- uptake rates

N_2 fixation and primary production (PP) were determined simultaneously from the same incubation sample at each depth in duplicate, using the ^{15}N-N_2 dissolution method (Großkopf et al., 2012) and ^{13}C-$NaHCO_3$ tracer addition technique (Hama et al., 1983), respectively. Details concerning the applied $^{15}N_2$ dissolution method can be found in Fonseca-Batista et al. (2017). Briefly, $^{15}N_2$-enriched seawater was prepared by degassing prefiltered (0.2 µm) low nutrient seawater, under acid-clean conditions using a peristaltic pump slowly circulating (100 mL min^{-1}) the seawater through two degassing membrane contactor systems (MiniModule, Liqui-Cel) in series, held under high vacuum (50 mbar). The degassed water was directly transferred into 2 L gastight Tedlar bags (Sigma-Aldrich) fitted with a septum through which 30 mL of pure $^{15}N_2$ gas (98 ^{15}N atom%, Eurisotop, lot number 23/051301) was injected before the bags were shaken 24 hours for tracer equilibration. This $^{15}N_2$ gas batch was previously shown to be free of ^{15}N-labelled contaminants such as nitrate, nitrite, ammonium and nitrous oxide (Fonseca-Batista et al., 2017). Each PC incubation bottle was partially filled with sampled seawater, then amended with 250 mL of $^{15}N_2$-enriched seawater and spiked with 3 mL of ^{13}C-labelled dissolved inorganic carbon (DIC; 200 mmol L^{-1} solution of $NaH^{13}CO_3$, 99%, Eurisotop). The ^{13}C-DIC added to a 4.5 L incubation bottle results in a ~6.5% increment of the initial DIC content, considered equal to the average oceanic DIC concentration (~2000 µmol kg^{-1}; Zeebe and Wolf-Gladrow, 2003). This allows sufficient tracer enrichment for a sensitive detection in the particulate organic carbon (POC) pool as a result of incorporation (Hama et al., 1983). Finally, each incubation bottle was topped off with the original seawater sample. Samples were then incubated for 24 hours in on-deck incubators circulated with surface seawater and wrapped with neutral density screens (Rosco) simulating the in situ irradiance conditions. After incubation, water was transferred under helium pressure from each PC bottle into triplicate 12 mL gastight Exetainer vials (Labco) poisoned (100 µL of saturated $HgCl_2$ solution) and pre-flushed with helium for the determination of the ^{15}N and ^{13}C atom% enrichments of the dissolved N_2 (in duplicate) and DIC pools. The remaining incubated sample was filtered onto pre-combusted MGF filters (glass microfiber filters, 0.7 µm nominal pore size, Sartorius), which were subsequently dried at 60 °C and stored at room temperature. The natural concentration and isotopic composition of POC and particulate nitrogen (PN) were assessed by filtering immediately after sampling an additional 4.5 L of non-spiked seawater from each depth. All samples were measured for POC and PN concentrations and isotopic compositions using an elemental analyser (EuroVector Euro EA 3000) coupled to an isotope ratio mass spectrometer (Delta V Plus, Thermo Scientific) and calibrated against international certified reference materials (CRM): IAEA-N1 and IAEA-305B for N and IAEA-CH6 and IAEA-309B for C. The isotopic composition of the DIC and dissolved N_2 pools was determined using a gas bench system coupled to an IRMS (Nu Instruments Perspective). Exetainers vials

were first injected with He to create a 4 mL headspace and then equilibrated on a rotatory shaker: for 12 hours after phosphoric acid addition (100 µL, 99%, Sigma-Aldrich) for DIC analyses and only for an hour without acid addition for N_2 analyses. DIC measurements were corrected according to Miyajima et al. (1995) and $^{15}N_2$ enrichments were calibrated with atmospheric N_2. N_2 fixation and carbon uptake volumetric rates were computed as shown in Equation 1:

$$N_2 \text{ or } HCO_3^- \text{ uptake } rate \text{ (nmol } L^{-1}d^{-1} \text{or µmol } m^{-3}d^{-1}) = \frac{A_{PN\ or\ POC}^{final} - A_{PN\ or\ POC}^{t=0}}{A_{N_2\ or\ DIC} - A_{PN\ or\ POC}^{t=0}} \times \frac{[PN\ or\ POC]}{\Delta t} \quad (1)$$

where $A_{PN\ or\ POC}$ represents the ^{15}N or ^{13}C atom% excess of PN or POC, respectively, at the beginning (t =0) and end (final) of the incubation, while $A_{N_2\ orDIC}$ represents the ^{15}N or ^{13}C atom% excess of the dissolved inorganic pool (N_2 or DIC); and Δt represents the incubation period.

Depth-integrated rates were calculated by non-uniform gridding trapezoidal integration for each station. The DL, defined as the minimal detectable uptake rates were determined as detailed in Fonseca-Batista et al. (2017). To do so, the minimal acceptable ^{15}N or ^{13}C enrichment of PN or POC after incubation (Montoya et al., 1996) is considered to be equal to the natural isotopic composition, specific to each sampled depth, plus three times the uncertainty obtained for N and C isotopic analysis of CRM. All remaining experiment-specific terms are then used to recalculate the minimum detectable uptake. Carbon uptake rates were always above their specific DL, while N_2 fixation was not detectable at any of the four depths of stations Bel-3 and Bel-5, nor at Bel-9 120 m, Bel-11 45 m and Geo-21 18 m (see Supporting Information Table S1).

2.4 DNA sampling and *nifH* diversity analysis

During the BG2014/14 and GEOVIDE cruises, water samples were also collected for DNA extraction and *nifH* sequencing at the stations where N_2 fixation rate measurements were carried out. Two liters of seawater samples were vacuum filtered (20 to 30 kPa) through sterile 0.2 µm 47 mm membrane filters (cellulose acetate Sartorius type 111 for BG2014/14; Millipore's Isopore - GTTP04700 for GEOVIDE) subsequently placed in cryovials directly flash deep frozen in liquid nitrogen. At the land-based laboratory samples were transferred to a –80 °C freezer until nucleic acid extraction.

For the BG2014/14 samples, DNA was extracted from the samples using the Power Water DNA Isolation kit (MOBIO) and checked for integrity by agarose gel electrophoresis. The amplification of *nifH* sequences was performed on 3–50 ng μL^{-1} environmental DNA samples using one unit of Taq polymerase (5PRIME), by nested PCR according to Zani et al. (2000) and Langlois et al. (2005). Amplicons of the predicted 359-bp size observed by gel electrophoresis were cloned using the PGEM T Easy cloning kit (PROMEGA) according to the manufacturer's instructions. A total of 103 clones were sequenced by the Sanger technique (GATC, Marseille).

For the GEOVIDE samples, DNA was extracted using the QIAGEN DNeasy Plant Mini Kit as instructed by the manufacture, with a modified step to improve cell lysis. This step consisted of an incubation at 52 °C on an orbital shaker for 1 hour (300 rpm) with 50 µL of lysozyme solution (5 mg mL^{-1} in TE buffer), 45 µL of Proteinase K solution (20 mg mL^{-1} in MilliQ PCR grade water) and 400 µL of AP1 lysis buffer from the QIAGEN DNeasy Plant Mini Kit. DNA concentration and purity were assessed with NanoDrop 2000 and then stored at -80 °C. The DNA samples were screened for the presence of the *nifH* gene as described in Langlois et al. (2005). Samples that tested positive were further prepared for next generation sequencing on an Illumina MiSeq platform using primers that included the nifH1/2 primers (Langlois et al., 2005; Ratten, 2017) attached to Illumina adaptors and barcodes for multiplexing in the Illumina MiSeq instrument. Next generation sequencing was carried out at the Integrated

Microbiome Resource (IMR) of the Centre for Comparative and Evolutionary Biology (CGEB) at Dalhousie University (Halifax, Canada). Raw Illumina paired-end reads of *nifH* were preprocessed using the QIIME pipeline (Quantitative Insights Into Microbial Ecology; Caporaso et al., 2010) following the IMR workflow (https://github.com/mlangill/microbiome_helper/wiki/16S-standard-operating-procedure; Comeau et al., 2017). The 28 OTUs for the *nifH* genes presented in this study were assembled based on 96% identity of sequence reads.

DNA alignments were performed using the Molecular Evolutionary Genetics Analysis software (MEGA 7.0) (Kumar et al., 2016) and *nifH* operational taxonomic units (*nifH*-OTUs) were defined with a maximum 5% divergence cut-off. DNA sequences were translated into amino acid sequences, then *nifH* evolutionary distances considered as the number of amino acid substitutions per site, were computed using the Poisson correction method (Nei, 1987). All positions containing gaps and missing data were eliminated (see phylogenetic tree in Fig. 6). One representative sequence of each *nifH*-OTU was deposited in GenBank under the accession numbers referenced from KY579322 to KY579337, for the Belgica DNA samples and referenced from MH974781 to MH974795 for the GEOVIDE Iberian samples.

2.5 Statistical analysis

The relationship between N_2 fixation activities and ambient physical and chemical properties was examined, using SigmaPlot (Systat Software, San Jose, CA) by computing Spearman rank correlation coefficients linking depth-integrated rates and volumetric rates of N_2 fixation and primary production to environmental variables. These ambient variables were either averaged or integrated over the euphotic layer, or considered as discrete measurements. These variables include temperature, salinity, Chl *a*, NH_4^+, NO_3^-+NO_2^-, phosphorus excess ($P^* = [PO_4^{3-}] - [NO_3^- + NO_2^-] / 16$) derived from in situ nutrient measurements and climatological data (Garcia et al., 2013), dissolved iron concentrations determined for the GEOVIDE cruise (Tonnard et al., 2018) and satellite-derived dust deposition fluxes at the time of our study (Giovanni online data system). When nutrient concentrations were below the DL we used the DL value to run the correlation test. In addition, we ran a principal component analysis (PCA) using XLSTAT 2017 (Addinsoft, Paris, France, 2017) to get an overview of the interconnection between all the latter key variables with N_2 fixation at the time of our study. The output of the PCA are discussed in section 4.3.

3 Results

3.1 Ambient environmental settings

Surface waters of all the ENACWst stations showed a relatively strong stratification resulting from the progressive spring heating, with sea surface temperature (SST) ranging from 15.3 (Geo-13) to 17.2 °C (Bel-13). At the surface, nutrients were depleted ($NO_3^- + NO_2^- < 0.09$ µM in the upper 20 m; Fig. 2c, f) and Chl *a* concentrations were low (< 0.25 µg L^{-1}; Fig. 2a, d) but showed a subsurface maximum (between 0.5 and 0.75 µg L^{-1} at approximately 50 m), a common feature for oligotrophic open ocean waters. Amongst the ENACWst stations, station Geo-13 had a slightly higher nutrient content ($NO_3^- + NO_2^-$ = 0.7 µM) in the lower mixed layer depth (MLD) and a higher Chl *a* concentration (> 0.5 µg L^{-1} in the upper 35 m).

Surface waters at ENACWsp stations were less stratified (SST between 14.0 and 14.5 °C), were nutrient replete (surface $NO_3^- + NO_2^-$ ranging from 0.3 to 0.8 µM) and had a higher phytoplankton biomass (Chl *a* between 0.7 to 1.2 µg L^{-1} in the upper 30 m except for station Bel-5). Highest Chl *a* values were observed at station Bel-7 (44.6° N, 9.3° W), which appeared to be located within an anticyclonic mesoscale eddy as evidenced by the downwelling structure

detected in the Chl *a* and NO_3^- + NO_2^- profiles (Fig. 2a, c) at this location (as well as T and S sections, data not shown).

3.2 Primary production and satellite-based Chl *a* observations

Primary production (PP), estimated through the incorporation of enriched bicarbonate (^{13}C-$NaHCO_3$) into the POC pool, illustrated volumetric rates ranging from 7 to 3500 µmol C m^{-3} d^{-1} (see Supporting Information Table S1) and euphotic layer integrated rates ranging from 32 to 137 mmol C m^{-2} d^{-1} (Fig. 3a, b, and Supporting Information Table S2). PP was relatively homogenous in the Bay of Biscay (stations Bel-3, Bel-5 and Bel-7) and along the Iberian Margin (Bel-9, Bel-11, Bel-13 and Geo-1) with average rates ranging from 33 to 43 mmol C m^{-2} d^{-1}, except for station Bel-7 where it was slightly higher (52 mmol C m^{-2} d^{-1}; Fig. 3a, b, and Table S2), likely due to the presence of an anticyclonic mesoscale structure at this location. PP increased westwards away from the Iberian Peninsula, reaching highest values at stations Geo-13 and Geo-21 (79 and 135 mmol C m^{-2} d^{-1}, respectively; Fig. 3b), but also slightly higher on the Portuguese shelf (reaching 59 mmol C m^{-2} d^{-1} at Geo-2). These results are in the range of past measurements in this region for the same period of the year, ranging from 19 to 103 mmol C m^{-2} d^{-1} (Marañón et al., 2000; Fernández et al., 2005; Poulton et al., 2006; Fonseca-Batista et al., 2017). Area-averaged Chl *a* derived from satellite imagery for a time-period overlapping with ours (Giovanni online data system; Fig. 4a, b) revealed that post-bloom conditions prevailed at most sites (Bel-3 to Bel-13 and Geo-1 to Geo-13) while bloom conditions were still ongoing at station Geo-21 at the time of our study.

3.3 N_2 fixation and dominant diazotrophs at the sampling sites

Volumetric N_2 fixation rates were above the DL at 8 of the 10 stations sampled in this study (Bel-3 and Bel-5 being below the DL) and ranged from 0.7 to 65.4 nmol N L^{-1} d^{-1} (see Table S1), with areal rates ranging between 81 and 1533 µmol N m^{-2} d^{-1} (Fig. 3c, d, and Table S2).

We observed intense N_2 fixation activities at the two sites (Bel-11 and Bel-13) most affected by ENACWst (Fig. S1). At stations Bel-11 and Bel-13, volumetric rates of N_2 fixation ranged from 2.4 to 65.4 nmol N L^{-1} d^{-1}, with highest rates found at surface level (65.4 and 45.0 nmol N L^{-1} d^{-1}, respectively), while areal rates averaged 1533 and 1355 µmol N m^{-2} d^{-1}, respectively. N_2 fixation was detected at all four GEOVIDE stations. Shelf-influenced (Geo-1 and Geo-2) and open ocean (Geo-13) ENACWst sites, geographically close to Bel-11 and Bel-13, also displayed high N_2 fixation activities with volumetric rates ranging from 1.0 to 7.1 nmol N L^{-1} d^{-1} (Table S1) while depth-integrated rates averaged 141, 262 and 384 µmol N m^{-2} d^{-1}, respectively (Fig. 3c, d, and Table S2). Significant N_2 fixation rates were also measured at stations that exhibited the highest primary production rates, including Bel-7, Geo-13 and Geo-21 (Fig. 3). We computed the relative contribution of N_2 fixation to PP by converting N_2 fixation rates to carbon uptake using either the Redfield ratio of 6.6 or the determined median POC/PN ratio for natural particles (equivalent to the mean value of 6.3 ± 1.1, ± SD, n = 46; Table 1). N_2 fixation contributed to less than 2% of PP at the ENACWsp sites Bel-7 and Geo-21 and between 3 to 28% of PP at the ENACWst sites, except for station Bel-9 where it supported about 1% of PP.

Screening of the *nifH* genes from DNA samples collected during the BG2014/14 cruise, returned positive *nifH* presence at stations Bel-11 and Bel-13 that displayed the largest areal N_2 fixation rates. Cloning of the *nifH* amplicons found in surface waters (54% PAR level where volumetric rates of N_2 fixation were the highest) yielded 103 *nifH* sequences. No successful *nifH* amplifications were obtained at the other Belgica stations or depths where

diazotrophic activities were lower or undetectable. All the clones (n = 41) recovered from station Bel-11 were taxonomically assigned to a single OTU that had 99% identity at the nucleotide level and 100% similarity at the amino acid level with the symbiotic diazotrophic cyanobacteria UCYN-A1 or *Candidatus Atelocyanobacterium thalassa*, first characterized from station ALOHA in the North Pacific (Fig. 5a and 6) (Thompson et al., 2012). While the UCYN-A OTU also dominated the clones recovered from station Bel-13, fourteen additional *nifH* phylotypes affiliated with non-cyanobacterial diazotrophs were also recovered at that station (Fig. 5a and 6). Among these 15 OTUs, represented by a total of 62 sequenced clones, 45.2% of the sequences were affiliated to UCYN-A1 (identical to those found at Bel-11), and the rest to heterotrophic bacteria with 25.8% affiliated to Bacteroidetes, 19.3% to Firmicutes and 9.7% to Proteobacteria (Gamma-, Epsilon- and Delta-proteobacteria; Fig. 5a and 6). For the GEOVIDE cruise, *nifH* screening returned positive *nifH* presence at stations Geo-2, Geo-13 and Geo-21. Next generation sequencing of these amplicons yielded in total 21001 reads, with a range of 170 to 9239 *nifH* amplicons per sample, belonging exclusively to non-cyanobacterial diazotrophs, with the major affiliation to Verrucomicrobia, and Gamma-, Delta- and Alpha-proteobacteria, representing 54, 28, 15 and 1% of total *nifH* amplicons, respectively (Fig. 5b and 6). Members of a clade that has recently been characterized from the TARA expedition through metagenome assembled genomes of marine heterotrophic diazotrophs (Delmont et al., 2018), were found among the Gammaproteobacteria OTU types that dominated the community at station Geo-21.

3.4 Relationship between N_2 fixation rates and environmental variables

N_2 fixation activities were measured in surface waters characterized by relatively low SST (12.5–17.3 °C) and a wide range of dissolved inorganic nitrogen (DIN) concentrations (NO_3^- + NO_2^- from < 0.1 to 7.6 µM). Water column integrated N_2 fixation tended to increase with average surface water salinity (n = 10, $p < 0.05$, Table S3) but was inversely correlated to satellite-based dust deposition in May 2014, the month during which our sampling took place (n = 10, $p < 0.01$). Volumetric rates of N_2 fixation tended to increase with temperature (n = 46, $p < 0.01$, Table S4) and excess phosphorus concentration (only available for Belgica studied sites, n = 24, $p < 0.01$) while being negatively correlated to nitrate plus nitrite concentration (n = 46, $p < 0.01$).

4 Discussion

During two quasi-simultaneous expeditions to the Iberian Basin and the Bay of Biscay in May 2014 (38.8–46.5° N), we observed N_2 fixation activity in surface waters of most visited stations (except for the two northernmost sites in the Bay of Biscay). Our results are in support of other recent studies that have observed diazotrophic communities and significant N_2 fixation rates in marine environments departing from the previously established belief that diazotrophs are preferentially associated with warm oceanic water and low fixed-nitrogen concentrations (Needoba et al., 2007; Rees et al., 2009; Blais et al., 2012; Mulholland et al., 2012; Shiozaki et al., 2015). Although there is growing evidence that diazotrophs and their activity can extend geographically to temperate coastal and shelf-influenced regions, there still exist very few rate measurements at higher latitudes, especially in open waters. In the following sections we shall (1) discuss the significance of N_2 fixation in the Iberian Basin as well as its relation to primary productivity pattern and extend our view to the whole Atlantic Ocean, (2) provide information on the taxonomic affiliation of diazotrophs present at the time of our study, and (3) explore potential environmental conditions that may have supported this unexpectedly high diazotrophic activity in the Iberian Basin.

4.1 Significance of N_2 fixation in the temperate ocean

In the present study, we found surprisingly high N_2 fixation activities at most of the studied sites. Rates were exceptionally elevated at two open ocean stations located between 38.8 and 40.7° N at about 11° W (averaging 1533 and 1355 µmol N m^{-2} d^{-1} at stations Bel-11 and Bel-13, respectively; Fig. 3c, d, and Tables S1 and S2). Although N_2 fixation was not detected in the central Bay of Biscay (stations Bel-3 and Bel-5), rates recorded at all the other sites were relatively high, not only in shelf-influenced areas (141 and 262 µmol N m^{-2} d^{-1} at stations Geo-1 and Geo-2, respectively) but also in the open ocean (average activities between 81 and 384 µmol N m^{-2} d^{-1} at stations Bel-7, Bel-9, Geo-13 and Geo-21).

By fuelling the bioavailable nitrogen pool, N_2 fixation may support marine primary production (PP), but the extent of this contribution needs to be established for areas outside tropical and subtropical regions. PP rates measured here are of similar range if not slightly higher than those reported in earlier investigations in the Northeast Atlantic from subtropical to temperate waters (32 to 137 mmol C m^{-2} d^{-1} relative to 19 to 103 mmol C m^{-2} d^{-1}) (Marañón et al., 2000; Fernández et al., 2005; Poulton et al., 2006; Fonseca-Batista et al., 2017). However, the contribution of N_2 fixation to PP in the present work (1–28% of PP) reached values twice as high as those reported in other studies for the tropical and subtropical northeast Atlantic (contributions to PP ranging from < 1% to 12%) (Voss et al., 2004; Rijkenberg et al., 2011; Fonseca-Batista et al., 2017). This observation further questions the accepted premise that oligotrophic surface waters of tropical and subtropical regions are the key environment where diazotrophic activity significantly supports marine primary productivity (Capone et al., 2005; Luo et al., 2014). Nevertheless, it is important to keep in mind that our computation relies on the assumption that only photoautotrophic diazotrophs contribute to bulk N_2 fixation, which may not always be the case, particularly in the present study, where mostly heterotrophic diazotrophs were observed. However, it is likely that all the recently fixed-nitrogen ultimately becomes available for the whole marine autotrophic community.

Previous studies in the open waters of the Iberian Basin (35–50° N, east of 25° W) reported relatively lower N_2 fixation rates (from < 0.1 to 140 µmol N m^{-2} d^{-1}), regardless of whether the bubble-addition method (Montoya et al., 1996) or the dissolution method (Mohr et al., 2010; Großkopf et al., 2012) was used. However, these studies were carried out largely outside the bloom period, either during the late growing season (summer and autumn) (Moore et al., 2009; Benavides et al., 2011; Snow et al., 2015; Riou et al., 2016; Fonseca-Batista et al., 2017) or during winter (Rijkenberg et al., 2011; Agawin et al., 2014). In contrast, the present study took place in spring, during or just at the end of the vernal phytoplankton bloom. Differences in timing of these various studies and to a lesser extent, in methodologies (bubble-addition versus dissolution method) may explain the discrepancies in diazotrophic activity observed between our study and earlier works. Yet, the 20 months survey by Moreira-Coello et al. (2017) in nitrogen-rich temperate coastal waters in the southern Bay of Biscay, covering the seasonal spring bloom and upwelling pulses, did not reveal significant N_2 fixation activities: from 0.1 to 1.6 µmol N m^{-2} d^{-1} (up to 3 orders of magnitude lower than those reported here). However, unlike our study, this work was carried out not only using the bubble-addition method but also in an inner coastal system, as opposed to the mainly open waters investigated here, making it difficult to predict which variable or combination of variables caused the difference observed between the two studies.

Our maximal values recorded at stations Bel-11 and Bel-13 are one order of magnitude higher than maximal N_2 fixation rates reported further south for the eastern tropical and subtropical North Atlantic (reaching up to 360–424 µmol N m^{-2} d^{-1}) (Großkopf et al., 2012; Subramaniam et al., 2013; Fonseca-Batista et al., 2017). Besides these two highly active sites, N_2 fixation rates at the other studied locations (ranging between 81 and 384 µmol N m^{-2} d^{-1}) were still in the upper range of values reported for the whole eastern Atlantic region. Yet, conditions favouring N_2 fixation

are commonly believed to be met in tropical and subtropical regions where highest activities have mostly been measured, particularly in the eastern North Atlantic (e.g., higher seawater temperature, DIN limiting concentrations, excess phosphorus supply through eastern boundary upwelling systems) (Capone et al., 2005; Deutsch et al., 2007; Luo et al., 2014; Fonseca-Batista et al., 2017).

In the Atlantic Ocean, very high N_2 fixation rates up to ~1000 µmol N m^{-2} d^{-1} as observed here, have only been reported for temperate coastal waters of the Northwest Atlantic (up to 838 µmol N m^{-2} d^{-1}) (Mulholland et al., 2012) and for tropical shelf-influenced and mesohaline waters of the Caribbean and Amazon River plume (maximal rates ranging between 898 and 1600 µmol N m^{-2} d^{-1}) (Capone et al., 2005; Montoya et al., 2007; Subramaniam et al., 2008). Shelf and mesohaline areas have indeed been shown to harbour considerable N_2 fixation activity, not only in tropical regions (Montoya et al., 2007; Subramaniam et al. 2008) but also in waters extending from temperate to polar areas (Rees et al., 2009; Blais et al., 2012; Mulholland et al., 2012; Shiozaki et al., 2015). Yet, the environmental conditions leading to the high N_2 fixation rates in these regions are currently not well understood. For tropical mesohaline systems, the conditions proposed to drive such an intense diazotrophic activity include the occurrence of highly competitive diatom-diazotrophs associations and the influence of excess phosphorus input (i.e., excess relative to the canonical Redfield P/N ratio; expressed as P*) from the Amazon River (Subramaniam et al., 2008). However, such conditions of excess P were not observed in previous studies carried out in high latitude shelf regions with elevated N_2 fixation activities (Blais et al., 2012; Mulholland et al., 2012; Shiozaki et al., 2015), nor was it distinctly apparent in the present study (see section 4.3). In addition, while tropical mesohaline regions are characterized by the predominance of diatom-diazotroph associations (and filamentous *Trichodesmium* spp.), in temperate shelf areas the diazotrophic community is reported to be essentially dominated by UCYN-A and heterotrophic bacteria (Rees et al., 2009; Blais et al., 2012; Mulholland et al., 2012; Agawin et al., 2014; Shiozaki et al., 2015; Moreira-Coello et al., 2017).

4.2 Features of the diazotrophic community composition in the temperate North Atlantic

Our qualitative assessment of *nifH* diversity revealed a predominance of UCYN-A symbionts, only at the two stations with the highest surface N_2 fixation rates (up to 65.4 and 45.0 nmol N L^{-1} d^{-1} at Bel-11 and Bel-13, respectively; Table S1) while the remaining *nifH* sequences recovered belonged to heterotrophic diazotrophs, at Bel-13 as well as at all the other sites where *nifH* genes could be detected. No *Trichodesmium nifH* sequences were recovered from either BG2014/14 or GEOVIDE DNA samples, and the absence of the filamentous cyanobacteria was also confirmed by the CHEMTAX analysis of phytoplankton pigments (M. Tonnard, personal communication, January 2018). Previous work in temperate regions of the global ocean, including the Iberian Margin also reported that highest N_2 fixation activities were predominantly related to the presence of UCYN-A symbionts, followed by heterotrophic bacteria, while *Trichodesmium* filaments were low or undetectable (Needoba et al., 2007; Rees et al., 2009; Mulholland et al., 2012; Agawin et al., 2014; Shiozaki et al., 2015; Moreira-Coello et al., 2017).

UCYN-A (in particular from the UCYN-A1 clade) were shown to live in symbioses with single-celled prymnesiophyte algae (Thompson et al., 2012). This symbiotic association, considered obligate, has been reported to be particularly abundant in the central and eastern basin of the North Atlantic (Rees et al., 2009; Krupke et al., 2014; Cabello et al., 2015; Martínez-Pérez et al., 2016).

Besides UCYN-A, all the remaining *nifH* sequences recovered from both cruises, although obtained through different approaches, belonged to non-cyanobacterial diazotrophs. The phylogenetic tree (Fig. 6) showed that the non-cyanobacterial diazotrophs clustered with (1) Verrucomicrobia, a phylum yet poorly known that includes aerobic to

microaerophilic methanotrophs groups, found in a variety of environments (Khadem et al., 2010; Wertz et al., 2012), (2) anaerobic bacteria, obligate or facultative, mostly affiliated to Cluster III phylotypes of functional nitrogenase (e.g., Bacteriodetes, Firmicutes, Proteobacteria) and lastly (3) phylotypes from Clusters I, II, and IV (e.g., Proteobacteria and Firmicutes). Among the Cluster III phylotypes, Bacteroidetes are commonly encountered in the marine environment and are known as specialized degraders of organic matter that preferably grow attached to particles or algal cells (Fernández-Gómez et al., 2013). N_2 fixation activity has previously been reported in five Bacteroidetes strains including *Bacteroides graminisolvens*, *Paludibacter propionicigenes* and *Dysgonomonas gadei* (Inoue et al., 2015) which are the closest cultured relatives of the *nifH*-OTUs detected at station Bel-13 (Fig. 6). Anaerobic Cluster III phylotypes have been previously recovered from different ocean basins (Church et al., 2005; Langlois et al., 2005, 2008; Man-Aharonovich et al., 2007; Rees et al., 2009; Halm et al., 2012; Mulholland et al., 2012). These diazotrophs were suggested to benefit from anoxic microzones found within marine snow particles or zooplankton guts to fix N_2 thereby avoiding oxygenic inhibition of their nitrogenase enzyme (Braun et al., 1999; Church et al., 2005; Scavotto et al., 2015). Therefore, the bloom to early post-bloom conditions, prevailing during our study, were likely beneficial for the development of diazotrophic groups that depend on the availability of detrital organic matter or on the association with grazing zooplankton. In contrast, at the northernmost Geo-21 station, we observed a dominance of Gammaproteobacteria phylotypes belonging to a recently identified clade of marine diazotrophs within the Oceanospirillales (Delmont et al., 2018).

These observations tend to strengthen the idea that not only UCYN-A (Cabello et al., 2015; Martínez-Pérez et al., 2016) but also non-cyanobacterial diazotrophs (Halm et al., 2012; Shiozaki et al., 2014; Langlois et al., 2015) play a substantial role in oceanic N_2 fixation. Although it is possible to assign a broad taxonomic affiliation to classify the *nifH* genes, very little is known with respect to their physiology, their role in the ecosystem and the factors controlling their distribution, due to the lack of representative whole genome sequences and environmentally relevant strains available for experimentation (Bombar et al., 2016). While the widespread distribution of UCYN-A and non-cyanobacterial diazotrophs has been reported, their contribution to in situ activity remains poorly quantified.

4.3 Key environmental drivers of N_2 fixation

Environmental conditions that promote autotrophic and heterotrophic N_2 fixation activity in the ocean are currently not well understood (Luo et al, 2014). While heterotrophic diazotrophs would not be directly affected by the commonly recognized environmental controls of autotrophic diazotrophy such as solar radiation, seawater temperature and DIN, as they possess fundamentally different ecologies, the molecular and cellular processes for sustaining N_2 fixation activity would nevertheless require a supply of dFe and P (Raven, 1988; Howard & Rees, 1996; Mills et al., 2004; Snow et al., 2015). Besides the need for these critical inorganic nutrients, heterotrophic N_2 fixation was also recently shown to be highly dependent on the availability of organic matter (Bonnet et al., 2013; Rahav et al., 2013, 2016; Loescher et al., 2014).

Findings from the GEOVIDE cruise tend to support the hypothesis of a stimulating effect of organic matter availability on N_2 fixation activity at the time of our study. Lemaitre et al. (2018) report that surface waters (upper 100–120 m) of the Iberian Basin (stations Geo-1 and Geo-13) and the West European Basin (Geo-21) carried significant POC loads (POC of 166, 171 and 411 mmol C m^{-2}, respectively) with a dominant fraction of small size POC (the 1–53 µm size fraction; 75%, 92% and 64% of the total POC, respectively). Smaller cells, usually being slow-sinking particles, are more easily remineralized in surface waters (Villa-Alfageme et al., 2016). This is confirmed by the very low export efficiency (only 3 to 4% of euphotic layer integrated PP) observed at stations Geo-

13 and Geo-21, suggesting an efficient shallow remineralisation (Lemaitre et al., 2018). This availability of organic matter in the upper layers likely contributed to supplying remineralized P (organic P being generally more labile than other organic nutrients; Vidal et al., 1999, 2003) and to enhancing the residence time of dFe originating from atmospheric deposition due to the formation of organic ligands (Jickells, 1999; de Baar and de Jong, 2001; Sarthou et al., 2003).

P* values from the BG2014/14 cruise (Table S1) and the climatological P* data for the Iberian Basin (Garcia et al., 2013) do not exhibit a clear PO_4^{3-} excess in the region (P* ranging from –0.1 to 0.1 µmol L^{-1}; Fig. 1 and Tables S1 and S2). Nevertheless, Spearman rank correlations indicate that volumetric N_2 fixation rates were significantly correlated with the BG2014/14 shipboard P* values (n = 24, $p < 0.01$, Table S4), with stations Bel-11 and Bel-13 weighing heavily in this correlation. Without the data from these two sites (data not shown), the correlation between in situ P* and N_2 fixation rates is no longer significant (n= 16, $p = 0.163$), while P* becomes highly correlated with PP and Chl *a* (n = 16, $p = 0.0257$ and 0.016, respectively). This suggests that the effect of P* on N_2 fixation, although not clearly evident from absolute values, was most important at stations Bel-11 and Bel-13 but nonetheless existent at the other sites (Bel-7 and Bel-9). The occurrence of N_2 fixation in oligotrophic waters displaying weak P* values, depleted in DIN and PO_4^{3-} but replete in dFe might in fact reflect the direct use by diazotrophs of dissolved organic phosphorus (DOP). Indeed, according to Landolfi et al. (2015) diazotrophy ensures the supply of additional N and energy for the enzymatic mineralization of DOP (synthesis of extracellular alkaline phosphatase). Therefore, a likely enhanced DOP release towards the end of the spring bloom may have contributed to sustaining N_2 fixation in the studied region. Such DOP utilization has indeed been reported for various marine organisms, particularly diazotrophic cyanobacteria (Dyhrman et al., 2006; Dyhrman & Haley, 2006) and bacterial communities (Luo et al., 2009).

Supply routes of dFe to surface waters of the investigated area relied on lateral advection from the continental shelf (stations Geo-1 and Geo-2) (Tonnard et al., 2018), vertical mixing due to post-winter convection (Thuróczy et al., 2010; Rijkenberg et al., 2012; García-Ibáñez et al., 2015), and/or atmospheric dust deposition (dry + wet). Atmospheric deposition may have been particularly important for the area of stations Bel-11 and Bel-13 receiving warm and saline surface waters from the subtropics.

Atmospheric aerosol deposition determined during the GEOVIDE cruise (Shelley et al., 2017), as well as the satellite-based dust deposition (dry + wet) averaged over the month of May 2014 (Fig. S3b; Giovanni online satellite data system, NASA Goddard Earth Sciences Data and Information Services Center), reveal rather weak dust loadings over the investigated region, resulting in areal N_2 fixation rates being actually inversely correlated to the satellite-based average dust input ($p < 0.01$, Table S3). In contrast, satellite-based dust deposition (dry + wet) averaged over the month of April 2014 (i.e. preceding the timing of sampling) indicates high fluxes over the subtropical waters located south of the studied region (Fig. S3a;). The θ/S diagrams at stations Bel-11 and Bel-13 (and to a lesser extent at Geo-13; Fig. S1) illustrate the presence of very warm and saline waters, which were advected from the subtropics as suggested by the satellite SST images (Fig. S2). We thus argue that advection of surface waters from south of the study area represented a source of atmospherically derived dFe and contributed to driving the high N_2 fixation activity recorded at stations Bel-11 and Bel-13. This resulted in N_2 fixation rates there being positively (although weakly) correlated ($p = 0.45$, Table S3) with the April average dust input.

For the central Bay of Biscay, where N_2 fixation was below the DL (stations Bel-3 and Bel-5), dust deposition in April 2014 was also the lowest, suggesting that N_2 fixation there might have been limited by dFe availability. Indeed, at stations Bel-3 and Bel-5 diazotrophic activity in surface waters was boosted following dFe amendments (> 25 nmol N L^{-1} d^{-1}; Li et al., 2018).

Thus, the enhanced N_2 fixation activity at stations Bel-11 and Bel-13, as compared to the other sites, was likely stimulated by the combined effects of the presence of highly competitive prymnesiophyte-UCYN-A symbionts, organic matter as a source of DOP, positive P* signatures and advection of subtropical surface waters enriched in dFe.

These statements are further supported by the outcome of a multivariate statistical analysis, providing a comprehensive view of the environmental features influencing N_2 fixation. A principal component analysis (PCA; Fig. 7 and Tables S2 and S5) generated two components (or axes) explaining 68% of the system's variability. Axis 1 illustrates the productivity of the system, or more precisely the oligotrophic state towards which it was evolving. Axis 1 is defined by a strong positive relation with surface temperature (reflecting the onset of stratification, particularly for stations Bel-11 and Bel-13; Fig. 7) and an inverse relation with PP and associated variables (Chl *a*, NH_4^+, NO_3^- + NO_2^-), which reflects the prevailing post-bloom conditions of the system. Sites characterized by a moderate (Bel-3 and Bel-5) to high (Bel-7, Geo-21 and to a lesser extent Geo-13) PP appear indeed tightly linked to these PP-associated variables as illustrated in Fig. 7. Axis 2 is defined by the positive relation with surface salinity and P* (Fig. 7) and reflects the advection of surface waters of subtropical origin for stations Bel-11, Bel-13 and Geo-13. For stations Geo-1 and Geo-2, the inverse relation with surface salinity (Fig. 7) is interpreted to reflect fluvial inputs (Tonnard et al., 2018). Finally, this statistical analysis indicates that N_2 fixation activity was likely influenced by the two PCA components, tentatively identified as productivity (axis 1) and surface water advection (axis 2) from the shelf and the subtropical region.

5 Conclusions

The present work highlights the occurrence of elevated N_2 fixation activities (81–1533 µmol N m^{-2} d^{-1}) in spring 2014 in open waters of the temperate eastern North Atlantic, off the Iberian Peninsula. These rates exceed those reported by others for the Iberian Basin, but which were largely obtained outside the bloom period (from < 0.1 to 140 µmol N m^{-2} d^{-1}). In contrast, we did not detect any N_2 fixation activity in the central Bay of Biscay. At sites where significant N_2 fixation activity was measured, rates were similar to or up to an order of magnitude larger than values reported for the eastern tropical and subtropical North Atlantic, regions commonly believed to represent the main areas harbouring oceanic N_2 fixation for the eastern Atlantic. Assuming that the carbon versus nitrogen requirements by these N_2 fixers obeyed the Redfield stoichiometry, N_2 fixation was found to contribute 1–3% of the euphotic layer daily PP and even up to 23–25% at the sites where N_2 fixation activities were the highest. The prymnesiophyte-symbiont *Candidatus* Atelocyanobacterium thalassa (UCYN-A) contributed the most to the *nifH* sequences recovered at the two sites where N_2 fixation activity were the highest, while the remaining sequences belonged exclusively to heterotrophic bacteria. We speculate that the unexpectedly high N_2 fixation activity recorded at the time of our study was sustained by (i) organic matter availability in these open waters, resulting from the prevailing vernal bloom to post-bloom conditions, in combination with (ii) excess phosphorus signatures which appeared to be tightly related to diazotrophic activity particularly at the two most active sites. Yet these observations and hypotheses rely on the availability of dFe with evidence for input from shelf waters and pulsed atmospheric dust deposition being a significant source of iron. Further studies are required to investigate this possible link between N_2 fixation activity and phytoplankton bloom under iron-replete conditions in the studied region and similar environments, as these would require to be considered in future assessment of global N_2 fixation.

Data availability. The data associated with the paper are available from the corresponding author upon request.

The Supplement related to this article is available.

Competing interests. The authors declare that they have no conflict of interest.

Acknowledgements. We thank the Captains and the crews of R/V *Belgica* and R/V *Pourquoi pas?* for their skilful logistic support. A very special thank goes to the chief scientists G. Sarthou and P. Lherminier of the GEOVIDE expedition for the great work experience and wonderful support on board. We would like to give special thanks to Pierre Branellec, Michel Hamon, Catherine Kermabon, Philippe Le Bot, Stéphane Leizour, Olivier Ménage (Laboratoire d'Océanographie Physique et Spatiale), Fabien Pérault and Emmanuel de Saint Léger (Division Technique de l'INSU, Plouzané, France) for their technical expertise during clean CTD deployments. We thank A. Roukaerts and D. Verstraeten for their assistance with laboratory analyses at the Vrije Universiteit Brussel. We acknowledge Ryan Barkhouse for the collection of the DNA samples during the GEOVIDE cruise, Jennifer Tolman and Jenni-Marie Ratten for the *nifH* amplification and Tag sequencing. P. Lherminer, P. Tréguer, E. Grossteffan, and M. Le Goff are gratefully acknowledged for providing us with the shipboard physico-chemical data including CTD and nitrate plus nitrite data from the GEOVIDE expedition. Shiptime for the Belgica BG2014/14 cruise was granted by Operational Directorate 'Natural Environment' (OD Nature) of the Royal Institute of Natural Sciences, Belgium. OD Nature (Ostend) is also acknowledged for their assistance in CTD operations and data acquisition on board the R/V *Belgica*. This work was financed by the Flanders Research Foundation (FWO contract G0715.12N) and Vrije Universiteit Brussel, R&D, Strategic Research Plan "Tracers of Past & Present Global Changes", and is a Belgian contribution to SOLAS. Additional funding was provided by the Fund for Scientific Research - FNRS (F.R.S.-FNRS) of the Wallonia-Brussels Federation (convention no. J.0150.15). X. Li was a FNRS doctorate Aspirant fellow (mandate no. FC99216). This study was also supported, through the GEOVIDE expedition, by the French National Research Agency (ANR-13-B506-0014), the Institut National des Sciences de L'Univers (INSU) of the Centre National de la Recherche Scientifique (CNRS), and the French Institute for Marine Science (Ifremer). This work was logistically supported for the by DT-INSU and GENAVIR. This publication is also a contribution to the Labex OT-Med [ANR-11-LABEX-0061, www.otmed.fr] funded by the « Investissements d'Avenir », French Government project of the French National Research Agency [ANR, www.agence-nationale-recherche.fr] through the A*Midex project [ANR-11-IDEX-0001-02], funding V. Riou during the preparation of the manuscript. Finally, this work was also supported by NSERC Discovery grant funding J. LaRoche.

References

Agawin, N. S. R., Benavides, M., Busquets, A., Ferriol, P., Stal, L. J. and Arístegui, J.: Dominance of unicellular cyanobacteria in the diazotrophic community in the Atlantic Ocean, Limnol. Oceanogr., 59(2), 623–637, doi:10.4319/lo.2014.59.2.0623, 2014.

Ambar, I. and Fiúza, A. F. G.: Some features of the Portugal Current System: a poleward slope undercurrent, an upwelling-related summer southward flow and an autumn-winter poleward coastal surface current, in: Proceedings of the Second International Conference on Air-Sea Interaction and on Meteorology and Oceanography of the

Coastal Zone, edited by: Katsaros, K. B., Fiúza, A. F. G. and Ambar, I., American Meteorological Society, Boston, Massachusetts, United States, 286-287, 1994.

Benavides, M., Agawin, N., Arístegui, J., Ferriol, P. and Stal, L.: Nitrogen fixation by Trichodesmium and small diazotrophs in the subtropical northeast Atlantic, Aquat. Microb. Ecol., 65(1), 43–53, doi:10.3354/ame01534, 2011.

Blais, M., Tremblay, J.-É., Jungblut, A. D., Gagnon, J., Martin, J., Thaler, M. and Lovejoy, C.: Nitrogen fixation and identification of potential diazotrophs in the Canadian Arctic, Global Biogeochem. Cycles, 26(3), 1–13, doi:10.1029/2011GB004096, 2012.

Bombar, D., Paerl, R. W. and Riemann, L.: Marine Non-Cyanobacterial Diazotrophs: Moving beyond Molecular Detection, Trends Microbiol., 24(11), 916–927, doi:10.1016/j.tim.2016.07.002, 2016.

Bonnet, S., Dekaezemacker, J., Turk-Kubo, K. A., Moutin, T., Hamersley, R. M., Grosso, O., Zehr, J. P. and Capone, D. G.: Aphotic N2 fixation in the Eastern Tropical South Pacific Ocean., PLoS One, 8(12), e81265, doi:10.1371/journal.pone.0081265, 2013.

Braun, S. T., Proctor, L. M., Zani, S., Mellon, M. T. and Zehr, J. P. Y.: Molecular evidence for zooplankton-associated nitrogen-fixing anaerobes based on amplification of the nifH gene, FEMS Microbiol. Ecol., 28, 273–279, 1999.

Breitbarth, E., Oschlies, A. and LaRoche, J.: Physiological constraints on the global distribution of Trichodesmium – effect of temperature on diazotrophy, Biogeosciences, 4, 53–61, doi:10.5194/bg-4-53-2007, 2007.

Cabello, A. M., Cornejo-Castillo, F. M., Raho, N., Blasco, D., Vidal, M., Audic, S., de Vargas, C., Latasa, M., Acinas, S. G. and Massana, R.: Global distribution and vertical patterns of a prymnesiophyte–cyanobacteria obligate symbiosis, ISME J., 1–14, doi:10.1038/ismej.2015.147, 2015.

Capone, D. G.: Trichodesmium, a Globally Significant Marine Cyanobacterium, Science, 276(5316), 1221–1229, doi:10.1126/science.276.5316.1221, 1997.

Capone, D. G., Burns, J. A., Montoya, J. P., Subramaniam, A., Mahaffey, C., Gunderson, T., Michaels, A. F. and Carpenter, E. J.: Nitrogen fixation by Trichodesmium spp.: An important source of new nitrogen to the tropical and subtropical North Atlantic Ocean, Global Biogeochem. Cycles, 19(2), 1–17, doi:10.1029/2004GB002331, 2005.

Caporaso, J. G., Kuczynski, J., Stombaugh, J., Bittinger, K., Bushman, F. D., Costello, E. K., Fierer, N., Peña, A. G., Goodrich, J. K., Gordon, J. I., Huttley, G. a, Kelley, S. T., Knights, D., Koenig, J. E., Ley, R. E., Lozupone, C. a, Mcdonald, D., Muegge, B. D., Pirrung, M., Reeder, J., Sevinsky, J. R., Turnbaugh, P. J., Walters, W. a, Widmann, J., Yatsunenko, T., Zaneveld, J. and Knight, R.: QIIME allows analysis of high- throughput community sequencing data Intensity normalization improves color calling in SOLiD sequencing, Nat. Publ. Gr., 7(5), 335–336, doi:10.1038/nmeth0510-335, 2010.

Church, M. J., Jenkins, B. D., Karl, D. M. and Zehr, J. P.: Vertical distributions of nitrogen-fixing phylotypes at Stn ALOHA in the oligotrophic North Pacific Ocean, Aquat. Microb. Ecol., 38(1), 3–14, doi:10.3354/ame038003, 2005.

Comeau, A. M., Douglas, G. M. and Langille, M. G. I.: Microbiome Helper: a Custom and Streamlined Workflow for Microbiome Research, mSystems, 2(1), e00127-16, doi:10.1128/mSystems.00127-16, 2017.

de Boyer Montégut, C., Madec, G., Fischer, A. S., Lazar, A., and Iudicone, D.: Mixed layer depth over the global ocean: An examination of profile data and a profile-based climatology. J. Geophys. Res., 109(12), 1–20. https://doi.org/10.1029/2004JC002378, 2004.

608 Delmont, T. O., Quince, C., Shaiber, A., Esen, Ö. C., Lee, S. T., Rappé, M. S., McLellan, S. L., Lücker, S. and Eren,
609 A. M.: Nitrogen-fixing populations of Planctomycetes and Proteobacteria are abundant in surface ocean
610 metagenomes, Nat. Microbiol., 3(8), 804–813, doi:10.1038/s41564-018-0209-4, 2018.
611 Deutsch, C., Sarmiento, J. L., Sigman, D. M., Gruber, N. and Dunne, J. P.: Spatial coupling of nitrogen inputs and
612 losses in the ocean., Nature, 445(7124), 163–167, doi:10.1038/nature05392, 2007.
613 Dore, J. E., Brum, J. R., Tupas, L. and Karl, D. M.: Seasonal and interannual variability in sources of nitrogen
614 supporting export in the oligotrophic subtropical North Pacific Ocean, Limnol. Ocean., 47(6), 1595–1607, 2002.
615 Dyhrman, S. T. and Haley, S. T.: Phosphorus scavenging in the unicellular marine diazotroph Crocosphaera watsonii
616 phosphorus scavenging in the unicellular marine diazotroph Crocosphaera watsonii, Appl. Environ. Microbiol.,
617 72(2), 1452–1458, doi:10.1128/AEM.72.2.1452, 2006.
618 Dyhrman, S. T., Chappell, P. D., Haley, S. T., Moffett, J. W., Orchard, E. D., Waterbury, J. B. and Webb, E. A.:
619 Phosphonate utilization by the globally important marine diazotroph Trichodesmium, Nature, 439(7072), 68–71,
620 doi:10.1038/nature04203, 2006.
621 Falkowski, P. G.: Evolution of the nitrogen cycle and its influence on the biological sequestration of CO2 in the
622 ocean, Nature, 387(6630), 272–275, doi:10.1038/387272a0, 1997.
623 Farnelid, H., Andersson, A. F., Bertilsson, S., Al-Soud, W. A., Hansen, L. H., Sørensen, S., Steward, G. F.,
624 Hagström, Å. and Riemann, L.: Nitrogenase gene amplicons from global marine surface waters are dominated by
625 genes of non-cyanobacteria, PLoS One, 6(4), doi:10.1371/journal.pone.0019223, 2011.
626 Farnelid, H., Bentzon-Tilia, M., Andersson, A. F., Bertilsson, S., Jost, G., Labrenz, M., Jürgens, K. and Riemann, L.:
627 Active nitrogen-fixing heterotrophic bacteria at and below the chemocline of the central Baltic Sea., ISME J., 7(7),
628 1413–23, doi:10.1038/ismej.2013.26, 2013.
629 Fernández-Gómez, B., Richter M, Schüler M, Pinhassi, J., Acinas, S., González, J. and Pedrós-Alió, C.: Ecology of
630 marine Bacteroidetes: a comparative genomics approach, ISME J., 7(5), 1026–1037, doi:10.1038/ismej.2012.169,
631 2013.
632 Fernández, A., Mouriño-Carballido, B., Bode, A., Varela, M. and Marañón, E.: Latitudinal distribution of
633 Trichodesmium spp. and N2 fixation in the Atlantic Ocean, Biogeosciences, 7(2), 3167–3176, doi:10.5194/bg-7-
634 3167-2010, 2010.
635 Fernández I., C., Raimbault, P., Garcia, N. and Rimmelin, P.: An estimation of annual new production and carbon
636 fluxes in the northeast Atlantic Ocean during 2001, J. Geophys. Res., 110(C7), 1–15, doi:10.1029/2004JC002616,
637 2005.
638 Fiúza, A.F.G.: Hidrologia e dinâmica das águas costeiras de Portugal (Hydrology and dynamics of the Portuguese
639 coastal waters), Ph.D. thesis, Universidade de Lisboa, Portugal, 294 pp., 1984.
640 Fonseca-Batista, D., Dehairs, F., Riou, V., Fripiat, F., Elskens, M., Deman, F., Brion, N., Quéroué, F., Bode, M. and
641 Auel, H.: Nitrogen fixation in the eastern Atlantic reaches similar levels in the Southern and Northern Hemisphere,
642 J. Geophys. Res. Ocean., 122, 4618–4632, doi:10.1002/2016JC012335, 2017.
643 Foster, R. A., Subramaniam, A., Mahaffey, C., Carpenter, E. J., Capone, D. G. and Zehr, J. P.: Influence of the
644 Amazon River plume on distributions of free-living and symbiotic cyanobacteria in the western tropical north
645 Atlantic Ocean, Limnol. Oceanogr., 52(2), 517–532, doi:10.4319/lo.2007.52.2.0517, 2007.
646 Frouin, R., Fiúza, A. F. G., Ambar, I. and Boyd, T. J.: Observations of a poleward surface current off the coasts of
647 Portugal and Spain during winter, J. Geophys. Res., 95(C1), 679, doi:10.1029/JC095iC01p00679, 1990.

García-Ibáñez, M. I., Pardo, P. C., Carracedo, L. I., Mercier, H., Lherminier, P., Ríos, A. F. and Pérez, F. F.: Structure, transports and transformations of the water masses in the Atlantic Subpolar Gyre, Prog. Oceanogr., 135, 18–36, doi:10.1016/j.pocean.2015.03.009, 2015.

Garcia, H. E., Locarnini, R. A., Boyer, T. P., Antonov, J. I., Baranova, O. K., Zweng, M. M., Reagan, J. R. and Johnson, D. R.: World Ocean Atlas 2013, Volume 4 : Dissolved Inorganic Nutrients (phosphate, nitrate, silicate), Silver Spring, Maryland, USA., 2013.

Grasshoff, K., Ehrhardt, M. and Kremling, K.: Methods of Seawater Analysis. Second, Revised and Extended Edition, Verlag Chemie GmbH, D-6940 Weinheim, Germany., 1983.

Großkopf, T., Mohr, W., Baustian, T., Schunck, H., Gill, D., Kuypers, M. M. M., Lavik, G., Schmitz, R. A., Wallace, D. W. R. and LaRoche, J.: Doubling of marine dinitrogen-fixation rates based on direct measurements, Nature, 488(7411), 361–364, doi:10.1038/nature11338, 2012.

Gruber, N.: The Marine Nitrogen Cycle: Overview and Challenges, in: Nitrogen in the Marine Environment, edited by: Capone, D. G., Bronk, D. A., Mulholland, M. M., Carpenter E. J., Academic Press, Cambridge, Massachusetts, United States, 1–50, https://doi.org/10.1016/B978-0-12-372522-6.X0001-1, 2008.

Halm, H., Lam, P., Ferdelman, T. G., Lavik, G., Dittmar, T., LaRoche, J., D'Hondt, S. and Kuypers, M. M. M.: Heterotrophic organisms dominate nitrogen fixation in the South Pacific Gyre., ISME J., 6(6), 1238–49, doi:10.1038/ismej.2011.182, 2012.

Hama, T., Miyazaki, T., Ogawa, Y., Iwakuma, T., Takahashi, M., Otsuki, A. and Ichimura, S.: Measurement of photosynthetic production of a marine phytoplankton population using a stable 13C isotope, Mar. Biol., 73, 31–36, 1983.

Holmes, R. M., Aminot, A., Kérouel, R., Hooker, B. A. and Peterson, B. J.: A simple and precise method for measuring ammonium in marine and freshwater ecosystems, Can. J. Fish. Aquat. Sci., 56(10), 1801–1808, doi:10.1139/f99-128, 1999.

Howard, J. B. and Rees, D. C.: Structural Basis of Biological Nitrogen Fixation., Chem. Rev., 96(7), 2965–2982, doi:10.1021/cr9500545, 1996.

Inoue, J., Oshima, K., Suda, W., Sakamoto, M., Iino, T., Noda, S., Hongoh, Y., Hattori, M. and Ohkuma, M.: Distribution and evolution of nitrogen fixation genes in the phylum Bacteroidetes., Microbes Environ., 30(1), 44–50, doi:10.1264/jsme2.ME14142, 2015.

Jickells, T. D.: The inputs of dust derived elements to the Sargasso Sea; a synthesis, Mar. Chem., 68(1–2), 5–14, doi:10.1016/S0304-4203(99)00061-4, 1999.

Khadem, A. F., Pol, A., Jetten, M. S. M. and Op Den Camp, H. J. M.: Nitrogen fixation by the verrucomicrobial methanotroph "Methylacidiphilum fumariolicum" SolV, Microbiology, 156(4), 1052–1059, doi:10.1099/mic.0.036061-0, 2010.

Kimura, M.: A simple method for estimating evolutionary rates of base substitutions through comparative studies of nucleotide sequences, J. Mol. Evol., 16(2), 111–120, doi:10.1007/BF01731581, 1980.

Krupke, A., Lavik, G., Halm, H., Fuchs, B. M., Amann, R. I. and Kuypers, M. M. M.: Distribution of a consortium between unicellular algae and the N2 fixing cyanobacterium UCYN-A in the North Atlantic Ocean, Environ. Microbiol., 16(10), 3153–3167, doi:10.1111/1462-2920.12431, 2014.

Kumar, S., Stecher, G. and Tamura, K.: MEGA7: Molecular Evolutionary Genetics Analysis version 7.0 for bigger datasets., Mol. Biol. Evol., msw054, doi:10.1093/molbev/msw054, 2016.

Landolfi, A., Koeve, W., Dietze, H., Kähler, P. and Oschlies, A.: A new perspective on environmental controls, Geophys. Res. Lett., 42(May), 4482–2289, doi.org/10.1002/2015GL063756, 2015.

Langlois, R., Großkopf, T., Mills, M., Takeda, S. and LaRoche, J.: Widespread Distribution and Expression of Gamma A (UMB), an Uncultured, Diazotrophic, γ-Proteobacterial nifH Phylotype., PLoS One, 10(6), e0128912, doi:10.1371/journal.pone.0128912, 2015.

Langlois, R. J., LaRoche, J. and Raab, P. a: Diazotrophic Diversity and Distribution in the Tropical and Subtropical Atlantic Ocean Diazotrophic Diversity and Distribution in the Tropical and Subtropical Atlantic Ocean, Appl. Environ. Microbiol., 71(12), 7910–7919, doi:10.1128/AEM.71.12.7910, 2005.

Langlois, R. J., Hümmer, D. and LaRoche, J.: Abundances and distributions of the dominant nifH phylotypes in the Northern Atlantic Ocean, Appl. Environ. Microbiol., 74(6), 1922–1931, doi:10.1128/AEM.01720-07, 2008.

Lemaitre, N., Planchon, F., Planquette, H., Dehairs, F., Fonseca-Batista, D., Roukaerts, A., Deman, F., Tang, Y., Mariez, C. and Sarthou, G.: High variability of export fluxes along the North Atlantic GEOTRACES section GA01: Particulate organic carbon export deduced from the 234Th method, Biogeosciences Discuss., (April), 1–38, doi:10.5194/bg-2018-190, 2018.

Li, X., Fonseca-Batista, D., Roevros, N., Dehairs, F. and Chou, L.: Environmental and nutrient controls of marine nitrogen fixation, Prog. Oceanogr., 167(August), 125–137, doi:10.1016/j.pocean.2018.08.001, 2018.

Loescher, C. R., Großkopf, T., Desai, F. D., Gill, D., Schunck, H., Croot, P. L., Schlosser, C., Neulinger, S. C., Pinnow, N., Lavik, G., Kuypers, M. M. M., Laroche, J. and Schmitz, R. A.: Facets of diazotrophy in the oxygen minimum zone waters off Peru, ISME J., 8(11), 2180–2192, doi:10.1038/ismej.2014.71, 2014.

Luo, H., Benner, R., Long, R. a and Hu, J.: Subcellular localization of marine bacterial alkaline phosphatases., Proc. Natl. Acad. Sci. U. S. A., 106(50), 21219–21223, doi:10.1073/pnas.0907586106, 2009.

Luo, Y.-W., Doney, S. C., Anderson, L. A., Benavides, M., Berman-Frank, I., Bode, A., Bonnet, S., Boström, K. H., Böttjer, D., Capone, D. G., Carpenter, E. J., Chen, Y. L., Church, M. J., Dore, J. E., Falcón, L. I., Fernández, A., Foster, R. A., Furuya, K., Gómez, F., Gundersen, K., Hynes, A. M., Karl, D. M., Kitajima, S., Langlois, R. J., LaRoche, J., Letelier, R. M., Marañón, E., McGillicuddy, D. J., Moisander, P. H., Moore, C. M., Mouriño-Carballido, B., Mulholland, M. R., Needoba, J. A., Orcutt, K. M., Poulton, A. J., Rahav, E., Raimbault, P., Rees, A. P., Riemann, L., Shiozaki, T., Subramaniam, A., Tyrrell, T., Turk-Kubo, K. A., Varela, M., Villareal, T. A., Webb, E. A., White, A. E., Wu, J. and Zehr, J. P.: Database of diazotrophs in global ocean: abundance, biomass and nitrogen fixation rates, Earth Syst. Sci. Data, 4(1), 47–73, doi:10.5194/essd-4-47-2012, 2012.

Luo, Y.-W., Lima, I. D., Karl, D. M., Deutsch, C. A. and Doney, S. C.: Data-based assessment of environmental controls on global marine nitrogen fixation, Biogeosciences, 11(3), 691–708, doi:10.5194/bg-11-691-2014, 2014.

Man-Aharonovich, D., Kress, N., Zeev, E. B., Berman-Frank, I. and Béjà, O.: Molecular ecology of nifH genes and transcripts in the eastern Mediterranean Sea, Environ. Microbiol., 9(9), 2354–2363, doi:10.1111/j.1462-2920.2007.01353.x, 2007.

Marañón, E., Holligan, P. M., Varela, M., Mouriño, B. and Bale, A. J.: Basin-scale variability of phytoplankton biomass, production and growth in the Atlantic Ocean, Deep Sea Res. Part I Oceanogr. Res. Pap., 47(5), 825–857, doi:10.1016/S0967-0637(99)00087-4, 2000.

Martínez-Pérez, C., Mohr, W., Löscher, C. R., Dekaezemacker, J., Littmann, S., Yilmaz, P., Lehnen, N., Fuchs, B. M., Lavik, G., Schmitz, R. A., LaRoche, J. and Kuypers, M. M. M.: The small unicellular diazotrophic symbiont, UCYN-A, is a key player in the marine nitrogen cycle, Nat. Microbiol., 1(September), 1–7, doi:10.1038/nmicrobiol.2016.163, 2016.

McCartney, M. S. and Talley, L. D.: The Subpolar Mode Water of the North Atlantic Ocean, J. Phys. Oceanogr., 12(11), 1169–1188, doi:10.1175/1520-0485(1982)012<1169:TSMWOT>2.0.CO;2, 1982.

Mills, M. M., Ridame, C., Davey, M., La Roche, J. and Geider, R. J.: Iron and phosphorus co-limit nitrogen fixation in the eastern tropical North Atlantic, Nature, 429(May), 292–294, doi:10.1038/nature02550, 2004.

Miyajima, T., Yamada, Y., Hanaba, Y. T., Yoshii, K., Koitabashi, K. and Wada, E.: Determining the stable isotope ratio of total dissolved inorganic carbon in lake water by GC/C/IRMS, Limnol. Oceanogr., 40(5), 994–1000, 1995.

Mohr, W., Großkopf, T., Wallace, D. W. R. and LaRoche, J.: Methodological underestimation of oceanic nitrogen fixation rates, PLoS One, 5(9), 1–7, doi:10.1371/journal.pone.0012583, 2010.

Montoya, J. P., Voss, M., Kahler, P. and Capone, D. G.: A Simple, High-Precision, High-Sensitivity Tracer Assay for N2 Fixation, Appl. Environ. Microbiol., 62(3), 986–993, 1996.

Montoya, J. P., Voss, M. and Capone, D. G.: Spatial variation in N2-fixation rate and diazotroph activity in the Tropical Atlantic, Biogeosciences, 4(3), 369–376, doi:10.5194/bg-4-369-2007, 2007.

Moore, C. M., Mills, M. M., Achterberg, E. P., Geider, R. J., LaRoche, J., Lucas, M. I., McDonagh, E. L., Pan, X., Poulton, A. J., Rijkenberg, M. J. A., Suggett, D. J., Ussher, S. J. and Woodward, E. M. S.: Large-scale distribution of Atlantic nitrogen fixation controlled by iron availability, Nat. Geosci., 2(12), 867–871, doi:10.1038/ngeo667, 2009.

Moreira-Coello, V., Mouriño-Carballido, B., Marañón, E., Fernández-Carrera, A., Bode, A. and Varela, M. M.: Biological N2 Fixation in the Upwelling Region off NW Iberia: Magnitude, Relevance, and Players, Front. Mar. Sci., 4(September), doi:10.3389/fmars.2017.00303, 2017.

Mulholland, M. R., Bernhardt, P. W., Blanco-Garcia, J. L., Mannino, A., Hyde, K., Mondragon, E., Turk, K., Moisander, P. H. and Zehr, J. P.: Rates of dinitrogen fixation and the abundance of diazotrophs in North American coastal waters between Cape Hatteras and Georges Bank, Limnol. Oceanogr., 57(4), 1067–1083, doi:10.4319/lo.2012.57.4.1067, 2012.

Needoba, J. A., Foster, R. A., Sakamoto, C., Zehr, J. P. and Johnson, K. S.: Nitrogen fixation by unicellular diazotrophic cyanobacteria in the temperate oligotrophic North Pacific Ocean, Limnol. Oceanogr., 52(4), 1317–1327, doi:10.4319/lo.2007.52.4.1317, 2007.

Nei, M.: Molecular Evolutionary Genetics, Columbia University Press, New York, United States, 1987.

Ohlendieck, U., Stuhr, A. and Siegmund, H.: Nitrogen fixation by diazotrophic cyanobacteria in the Baltic Sea and transfer of the newly fixed nitrogen to picoplankton organisms, J. Mar. Syst., 25(3–4), 213–219, doi:10.1016/S0924-7963(00)00016-6, 2000.

Poulton, A. J., Holligan, P. M., Hickman, A., Kim, Y. N., Adey, T. R., Stinchcombe, M. C., Holeton, C., Root, S. and Woodward, E. M. S.: Phytoplankton carbon fixation, chlorophyll-biomass and diagnostic pigments in the Atlantic Ocean, Deep. Res. Part II Top. Stud. Oceanogr., 53(14–16), 1593–1610, doi:10.1016/j.dsr2.2006.05.007, 2006.

Rahav, E., Bar-Zeev, E., Ohayon, S., Elifantz, H., Belkin, N., Herut, B., Mulholland, M. R. and Berman-Frank, I.: Dinitrogen fixation in aphotic oxygenated marine environments, Front. Microbiol., 4(AUG), 1–11, doi:10.3389/fmicb.2013.00227, 2013.

Rahav, E., Giannetto, M. J. and Bar-Zeev, E.: Contribution of mono and polysaccharides to heterotrophic N2 fixation at the eastern Mediterranean coastline, Sci. Rep., 6(May), 1–11, doi:10.1038/srep27858, 2016.

Ras, J., Claustre, H. and Uitz, J.: Spatial variability of phytoplankton pigment distributions in the Subtropical South Pacific Ocean: comparison between in situ and predicted data, Biogeosciences, 5, 353–369, doi:10.5194/bgd-4-3409-2007, 2008.

Ratten, J.-M.: The diversity, distribution and potential metabolism of non-cyanobacterial diazotrophs in the North Atlantic Ocean, Dalhousie University., 2017.

Ratten, J. M., LaRoche, J., Desai, D. K., Shelley, R. U., Landing, W. M., Boyle, E., Cutter, G. A. and Langlois, R. J.: Sources of iron and phosphate affect the distribution of diazotrophs in the North Atlantic, Deep. Res. Part II Top. Stud. Oceanogr., 116, 332–341, doi:10.1016/j.dsr2.2014.11.012, 2015.

Raven, J. A.: The iron and molybdenum use efficiencies of plant growth with different energy, carbon and nitrogen sources, New Phytol., 109, 279–287, doi:10.1111/j.1469-8137.1988.tb04196.x, 1988.

Rees, A., Gilbert, J. and Kelly-Gerreyn, B.: Nitrogen fixation in the western English Channel (NE Atlantic Ocean), Mar. Ecol. Prog. Ser., 374(1979), 7–12, doi:10.3354/meps07771, 2009.

Rijkenberg, M. J. A., Langlois, R. J., Mills, M. M., Patey, M. D., Hill, P. G., Nielsdóttir, M. C., Compton, T. J., LaRoche, J. and Achterberg, E. P.: Environmental forcing of nitrogen fixation in the Eastern Tropical and Sub-Tropical North Atlantic Ocean, PLoS One, 6(12), doi:10.1371/journal.pone.0028989, 2011.

Riou, V., Fonseca-Batista, D., Roukaerts, A., Biegala, I. C., Prakya, S. R., Magalhães Loureiro, C., Santos, M., Muniz-Piniella, A. E., Schmiing, M., Elskens, M., Brion, N., Martins, M. A. and Dehairs, F.: Importance of N2-Fixation on the Productivity at the North-Western Azores Current/Front System, and the Abundance of Diazotrophic Unicellular Cyanobacteria, PLoS One, 11(3), e0150827, doi:10.1371/journal.pone.0150827, 2016.

Sarthou, G., Baker, A. R., Blain, S., Achterberg, E. P., Boye, M., Bowie, A. R., Croot, P., Laan, P., De Baar, H. J. W., Jickells, T. D. and Worsfold, P. J.: Atmospheric iron deposition and sea-surface dissolved iron concentrations in the eastern Atlantic Ocean, Deep. Res. Part I Oceanogr. Res. Pap., 50(10–11), 1339–1352, doi:10.1016/S0967-0637(03)00126-2, 2003.

Scavotto, R. E., Dziallas, C., Bentzon-Tilia, M., Riemann, L. and Moisander, P. H.: Nitrogen-fixing bacteria associated with copepods in coastal waters of the North Atlantic Ocean, Environ. Microbiol., 17(10), 3754–3765, doi:10.1111/1462-2920.12777, 2015.

Shelley, R. U., Roca-Martí, M., Castrillejo, M., Sanial, V., Masqué, P., Landing, W. M., van Beek, P., Planquette, H. and Sarthou, G.: Quantification of trace element atmospheric deposition fluxes to the Atlantic Ocean (> 40°N; GEOVIDE, GEOTRACES GA01) during spring 2014, Deep. Res. Part I, 119(November 2016), 34–49, doi:10.1016/j.dsr.2016.11.010, 2017.

Shiozaki, T., Ijichi, M., Kodama, T., Takeda, S., Furuya, K., Ijichi, M., Kodama, T., Takeda, S. and Furuya, K.: Heterotrophic bacteria as major nitrogen fixers in the euphotic zone of the Indian Ocean, Global Biogeochem. Cycles, 28, 1096–1110, doi.org/10.1002/2014GB004886, 2014.

Shiozaki, T., Nagata, T., Ijichi, M. and Furuya, K.: Nitrogen fixation and the diazotroph community in the temperate coastal region of the northwestern North Pacific, Biogeosciences, 12(15), 4751–4764, doi:10.5194/bg-12-4751-2015, 2015.

Snow, J. T., Schlosser, C., Woodward, E. M. S., Mills, M. M., Achterberg, E. P., Mahaffey, C., Bibby, T. S. and Moore, C. M.: Environmental controls on the biogeography of diazotrophy and Trichodesmium in the Atlantic Ocean, Global Biogeochem. Cycles, 29, 865–884, doi.org/10.1002/2015GB005090, 2015.

Subramaniam, A., Yager, P. L., Carpenter, E. J., Mahaffey, C., Björkman, K., Cooley, S., Kustka, A. B., Montoya, J. P., Sañudo-Wilhelmy, S. A., Shipe, R. and Capone, D. G.: Amazon River enhances diazotrophy and carbon sequestration in the tropical North Atlantic Ocean, Global Biogeochem. Cycles, 105, 10460–10465, doi:10.1029/2006GB002751, 2008.

Subramaniam, A., Mahaffey, C., Johns, W. and Mahowald, N.: Equatorial upwelling enhances nitrogen fixation in the Atlantic Ocean, Geophys. Res. Lett., 40(9), 1766–1771, doi:10.1002/grl.50250, 2013.

Thompson, A. W., Foster, R. A., Krupke, A., Carter, B. J., Musat, N., Vaulot, D., Kuypers, M. M. M. and Zehr, J. P.: Unicellular Cyanobacterium Symbiotic with a Single-Celled Eukaryotic Alga, Science, 337(September), 1546–1550, 2012.

Thuróczy, C.-E., Gerringa, L. J. A., Klunder, M. B., Middag, R., Laan, P., Timmermans, K. R. and de Baar, H. J. W.: Speciation of Fe in the Eastern North Atlantic Ocean, Deep Sea Res. Part I Oceanogr. Res. Pap., 57(11), 1444–1453, doi:10.1016/j.dsr.2010.08.004, 2010.

Tonnard, M., Planquette, H., Bowie, A. R., van der Merwe, P., Gallinari, M., Deprez de Gesincourt, F., Germain, Y., Gourain, A., Benetti, M., Reverdin, G., Treguer, P., Boutorh, J., Cheize, M., Menzel Barraqueta, J.-L., Pereira-Contraira, L., Shelley, R., Lherminier, P. and Sarthou, G.: Dissolved iron distribution in the North Atlantic Ocean and Labrador Sea along the GEOVIDE section (GEOTRACES section GA01), Biogeosciences Discuss., (April), 2018.

Vidal, M., Duarte, C. M. and Agustí, S.: Dissolved organic nitrogen and phosphorus pools and fluxes in the central Atlantic Ocean, Limnol. Oceanogr., 44(1), 106–115, 1999.

Vidal, M., Duarte, C. M., Agustí, S., Gasol, J. M. and Vaqué, D.: Alkaline phosphatase activities in the central Atlantic Ocean indicate large areas with phosphorus deficiency, Mar. Ecol. Prog. Ser., 262, 43–53, doi:10.3354/meps262043, 2003.

Villa-Alfageme, M., de Soto, F. C., Ceballos, E., Giering, S. L. C., Le Moigne, F. A. C., Henson, S., Mas, J. L. and Sanders, R. J.: Geographical, seasonal, and depth variation in sinking particle speeds in the North Atlantic, Geophys. Res. Lett., 43, 8609–8616, doi.org/10.1002/2016GL069233, 2016.

Voss, M., Croot, P., Lochte, K., Mills, M. and Peeken, I.: Patterns of nitrogen fixation along 10°N in the tropical Atlantic, Geophys. Res. Lett., 31(23), 1–4, doi:10.1029/2004GL020127, 2004.

Wertz, J. T., Kim, E., Breznak, J. A., Schmidt, T. M. and Rodrigues, J. L. M.: Genomic and physiological characterization of the Verrucomicrobia isolate Diplosphaera colitermitum gen. nov., sp. nov., reveals microaerophily and nitrogen fixation genes, Appl. Environ. Microbiol., 78(5), 1544–1555, doi:10.1128/AEM.06466-11, 2012.

Yentsch, C. S. and Menzel, D. W.: A method for the determination of phytoplankton chlorophyll and phaeophytin by fluorescence, Deep Sea Res. Oceanogr. Abstr., 10(3), 221–231, doi:10.1016/0011-7471(63)90358-9, 1963.

Zani, S., Mellon, M. T., Collier, J. L. and Zehr, J. P.: Expression of nifH genes in natural microbial assemblages in Lake George, New York, detected by reverse transcriptase PCR, Appl. Environ. Microbiol., 66(7), 3119–3124, doi:10.1128/AEM.66.7.3119-3124.2000, 2000.

Zeebe, R. E. and Wolf-Gladrow, D.: CO2 in seawater: equilibrium, kinetics, isotopes, Elsevier Science, Amsterdam, The Netherlands., 2003.

844 **Tables**

845

846

847 **Table 1:** Relative contribution (%) of N_2 fixation to Primary Production (PP).

Province	Station	Latitude (° N)	Longitude (° E)	N_2 fixation contribution to PP (%) (Redfield 6.6 ratio)	SD	N_2 fixation contribution to PP (%) (mean POC/PN ratio of 6.3 ± 1.1)	SD
ENACWsp	**Bel-3**	46.5	-8.0	**0**	-	**0**	-
	Bel-5	45.3	-8.8	**0**	-	**0**	-
	Bel-7	44.6	-9.3	**2**	0.4	**1**	0.4
	Geo-21	46.5	-19.7	**1**	0.02	**1**	0.0
ENACWst	**Bel-9**	42.4	-9.7	**1**	0.1	**1**	0.1
	Bel-11	40.7	-11.1	**28**	1.9	**25**	1.8
	Bel-13	38.8	-11.4	**25**	1.3	**23**	1.2
	Geo-1	40.3	-10.0	**3**	0.2	**3**	0.1
	Geo-2	40.3	-9.5	**3**	0.1	**3**	0.1
	Geo-13	41.4	-13.9	**3**	0.1	**3**	0.1

848

Figure legends

Figure 1: Location of sampling stations during the Belgica BG2014/14 (black labels) and GEOVIDE (white labels) cruises (May 2014) superimposed on a map of the seasonal average phosphate excess ($P^* = [PO_4^{3-}] - [NO_3^-] / 16$) at 20 m (April to June for the period from 1955 to 2012; World Ocean Atlas 2013; Garcia et al., 2013). Areas of dominance of the Eastern North Atlantic Central Waters of subpolar (ENACWsp) and subtropical (ENACWst) origin are separated by a horizontal dashed line. Black dashed and solid contour lines illustrate 500 m and 1500 m isobaths, respectively. (Schlitzer, R., Ocean Data View).

Figure 2: Spatial distribution of Chl *a* **(a, d)**, NH_4^+ **(b, e)** and $NO_3^- + NO_2^-$ **(c, f)** concentrations along the Belgica BG2014/14 **(upper panels)** and GEOVIDE **(lower panels)** cruise tracks. Station numbers are indicated above the sections. The vertical black line represents the boundary between areas with dominance of Eastern North Atlantic Waters of subpolar (ENACWsp) and subtropical (ENACWst) origin. Mixed layer depth (MLD, black lines connecting diamonds) was estimated using a temperature threshold criterion of 0.2 °C relative to the temperature at 10 m (de Boyer Montégut et al., 2004). (Schlitzer, R., Ocean Data View).

Figure 3: Spatial distribution (± SD) of depth-integrated rates of primary production **(a, b)** (duplicates are in light and dark green bars with the corresponding values in mmol C m^{-2} d^{-1}); N_2 fixation **(c, d)** (duplicates are in light and dark blue bars with the corresponding values in µmol N m^{-2} d^{-1}) determined during the Belgica BG2014/14 **(a, c)** and GEOVIDE **(b, d)** cruises. Error bars represent the propagated measurement uncertainty of all parameters used to compute volumetric uptake rates.

Figure 4: Time series of area-averaged chlorophyll a concentration (mg m^{-3}) registered by Aqua MODIS satellite (Giovanni online satellite data system) between December 2013 and December 2014 for the 0.5° x 0.5° grid surrounding the different stations during the **(a)** Belgica BG2014/14 and **(b)** GEOVIDE cruises. The dashed box highlights the sampling period for both cruises (May 2014).

Figure 5: Diversity of *nifH* sequences during **(a)** the Belgica BG2014/14 cruise (successfully recovered only at stations Bel-11 and Bel-13, 5 m) and **(b)** the GEOVIDE cruise (stations Geo-2, 100 m; Geo-13, 35 m and Geo-21, 15 and 70 m. The total numbers of recovered sequences are indicated on top of the bars, and the exact percentage represented by each group is shown inside the bars.

Figure 6: Phylogenetic tree of *nifH* predicted amino acid sequences generated using the Maximum Likelihood method of the Kimura 2-parameter model (Kimura, 1980) via the Molecular Evolutionary Genetics Analysis software (MEGA 7.0) (Kumar et al., 2016). Initial tree(s) for the heuristic search were obtained automatically by applying Neighbor-Join and BioNJ algorithms to a matrix of pairwise distances estimated using the Maximum Composite Likelihood (MCL) approach, and then selecting the topology with superior log likelihood value. A discrete Gamma distribution was used to model evolutionary rate differences among sites (5 categories (+G, parameter = 0.4038)). All sequences recovered from DNA samples, including those previously identified and the newly recovered ones (with ≥ 95% similarity at the nucleotide level with representative clones) are highlighted in blue. For the *nifH* sequences recovered from the GEOVIDE cruise, only those contributing to the cumulative 98% of recovered sequences were included in this tree. Bootstrap support values (≥ 50%) for 100 replications are shown at nodes. The scale bar

890 indicates the number of sequence substitutions per site. The archaean *Methanobrevibacter smithii* was used as an
891 outgroup. Accession numbers for published sequences used to construct the phylogenetic tree are given.
892
893 **Figure 7:** Euclidean distance biplot illustrating the axis loadings for the two main PCA components based on the
894 Spearman rank correlation matrix shown in Table S3. Variables taken into account include depth-integrated rates of
895 N_2 fixation and primary production (PP), average phosphate excess at 20 m depth surrounding each sampled site
896 recovered from World Ocean Atlas 2013 climatology data between April and June from 1955 to 2012 (Garcia et al.,
897 2013); satellite average dust deposition (dry + wet) derived during April 2014 (Giovanni online data system, NASA
898 Goddard Earth Sciences Data and Information Services Center) and ambient variables (temperature, salinity, and
899 nutrient data). Coloured dots in the biplot represent the projection of the different stations. Axis 1 has high negative
900 loadings for PP, Chl *a*, NH_4^+ and $NO_3^- + NO_2^-$, and high positive loadings for temperature and N_2 fixation rates, with
901 values of –0.812, –0.768, –0.936, –0.783, 0.942 and 0.506, respectively (see Table S5). Axis 2 has high positive
902 loadings of 0.584, 0.943 and 0.602 for climatological P*, salinity and N_2 fixation rates, respectively. PCA analysis
903 was run in XLSTAT 2017 (Addinsoft, Paris, France, 2017).

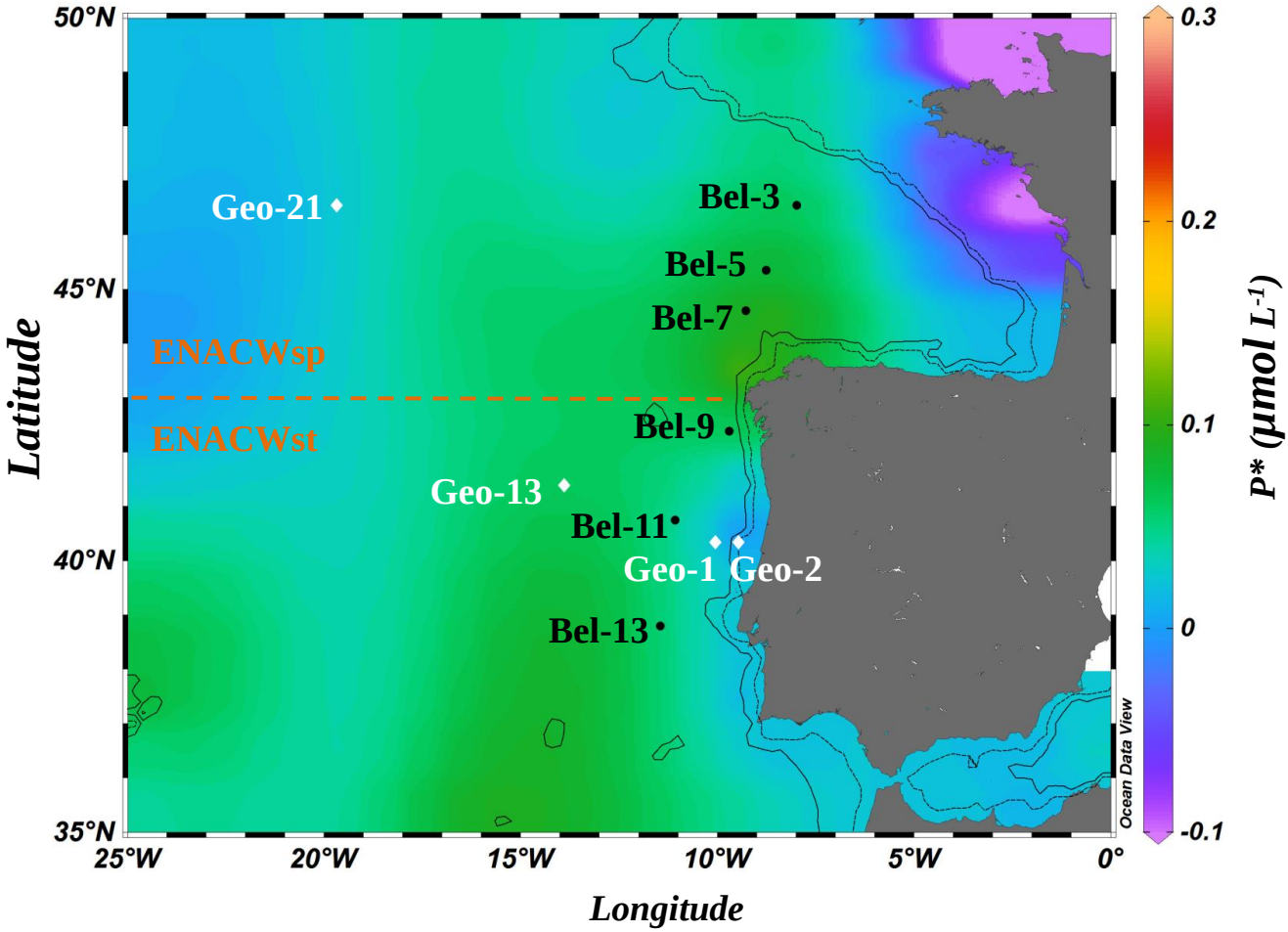
50°N
45°N
40°N
35°N
25°W
20°W
15°W
10°W
5°W
0°
Latitude
Longitude
Geo-21
Bel-3
Bel-5
Bel-7
ENACWsp
ENACWst
Bel-9
Geo-13
Bel-11
Geo-1
Geo-2
Bel-13
0.3
0.2
0.1
0
-0.1
P* (µmol L-1)
Ocean Data View

Figure 1

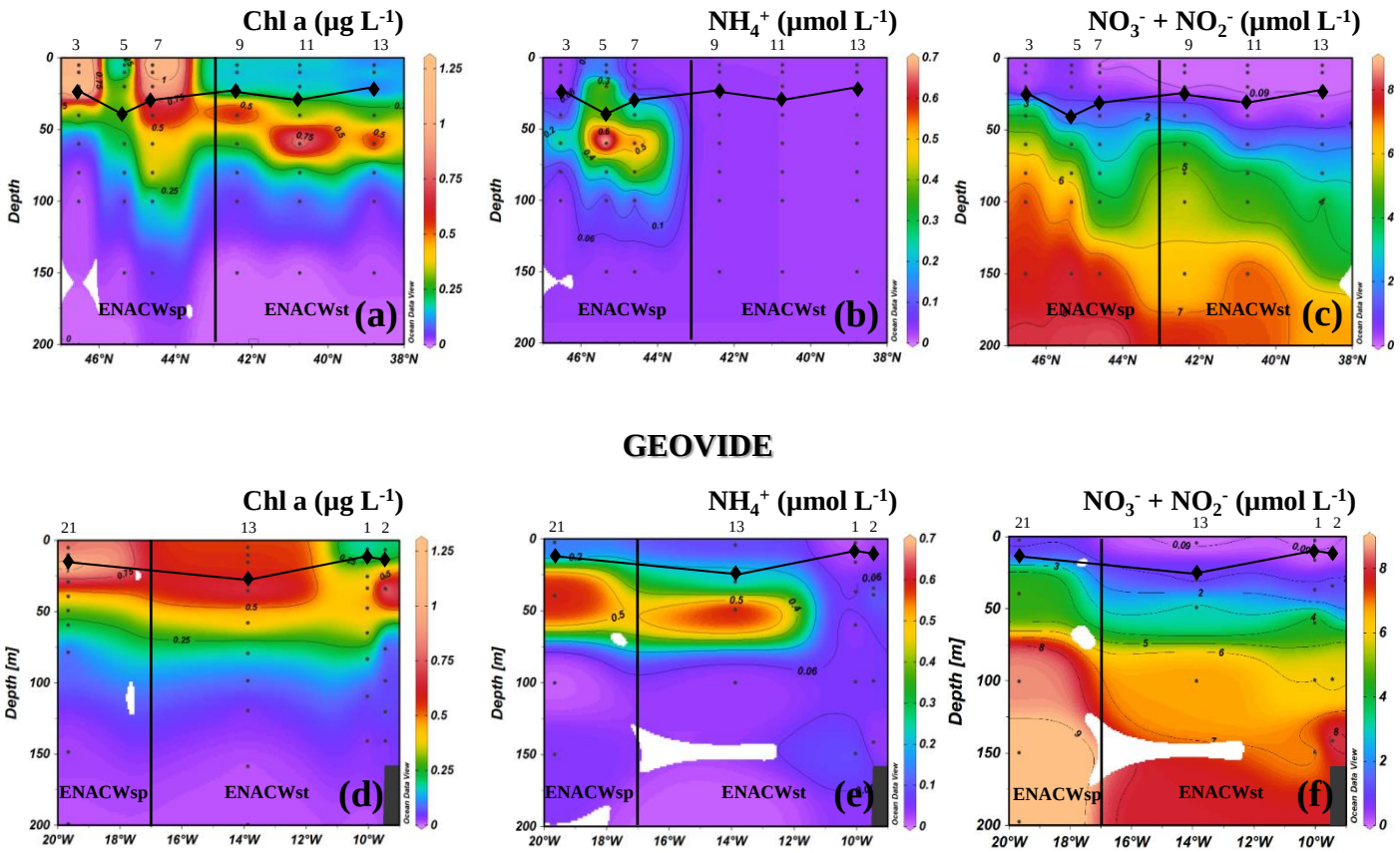
Belgica BG2014/14
Chl a (µg L-1)
NH4+ (µmol L-1)
NO3- + NO2- (µmol L-1)
Depth
ENACWsp
ENACWst
(a)
(b)
(c)
GEOVIDE
Chl a (µg L-1)
NH4+ (µmol L-1)
NO3- + NO2- (µmol L-1)
Depth [m]
ENACWsp
ENACWst
(d)
(e)
(f)

Figure 2

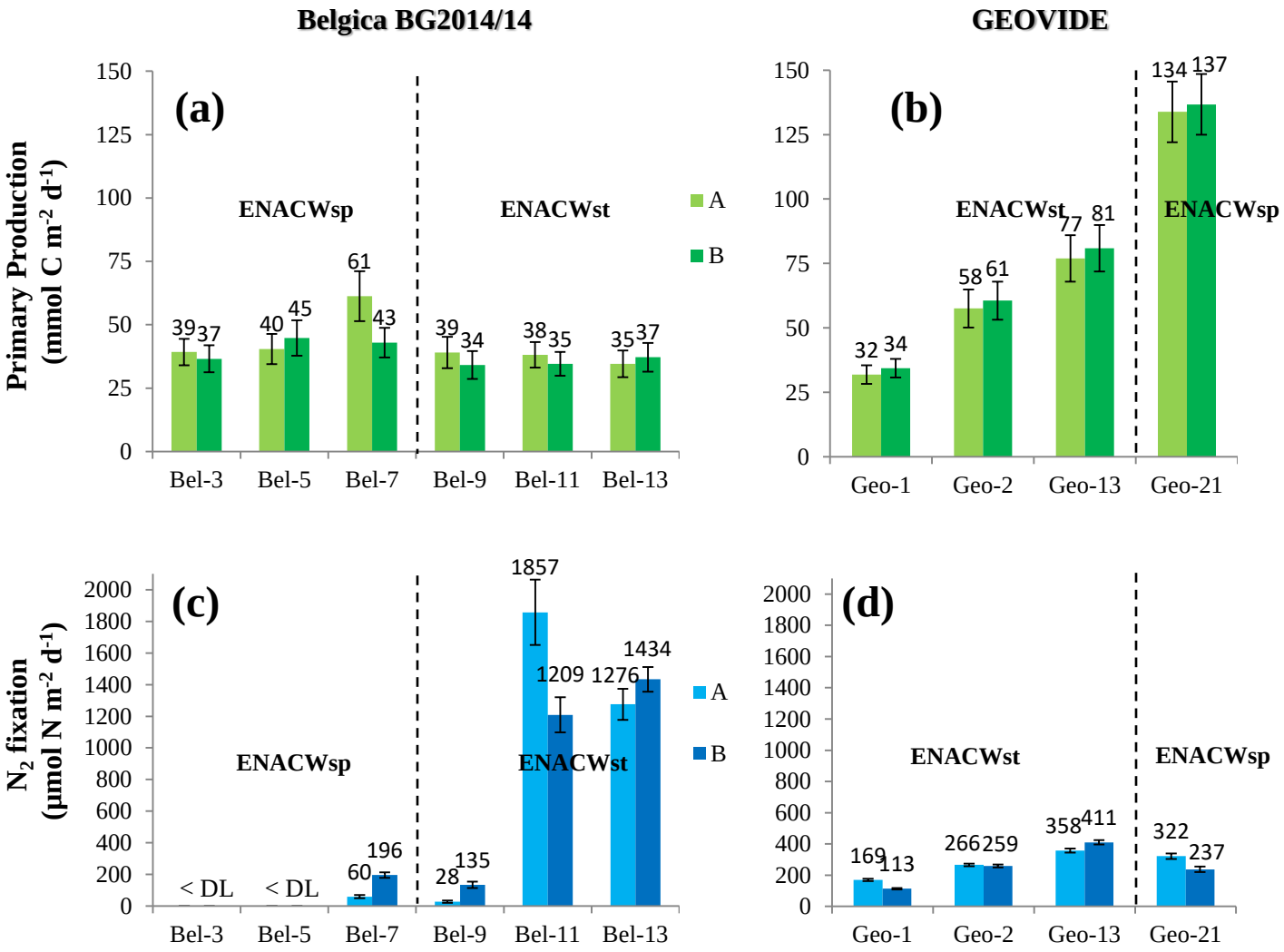
Belgica BG2014/14
GEOVIDE
(a)
(b)
(c)
(d)
Primary Production (mmol C m-2 d-1)
N2 fixation (µmol N m-2 d-1)
ENACWsp
ENACWst
A
B
Bel-3
Bel-5
Bel-7
Bel-9
Bel-11
Bel-13
Geo-1
Geo-2
Geo-13
Geo-21
< DL
< DL
39 37
40 45
61 43
39 34
38 35
35 37
32 34
58 61
77 81
134 137
60 196
28 135
1857 1209
1276 1434
169 113
266 259
358 411
322 237

Figure 3

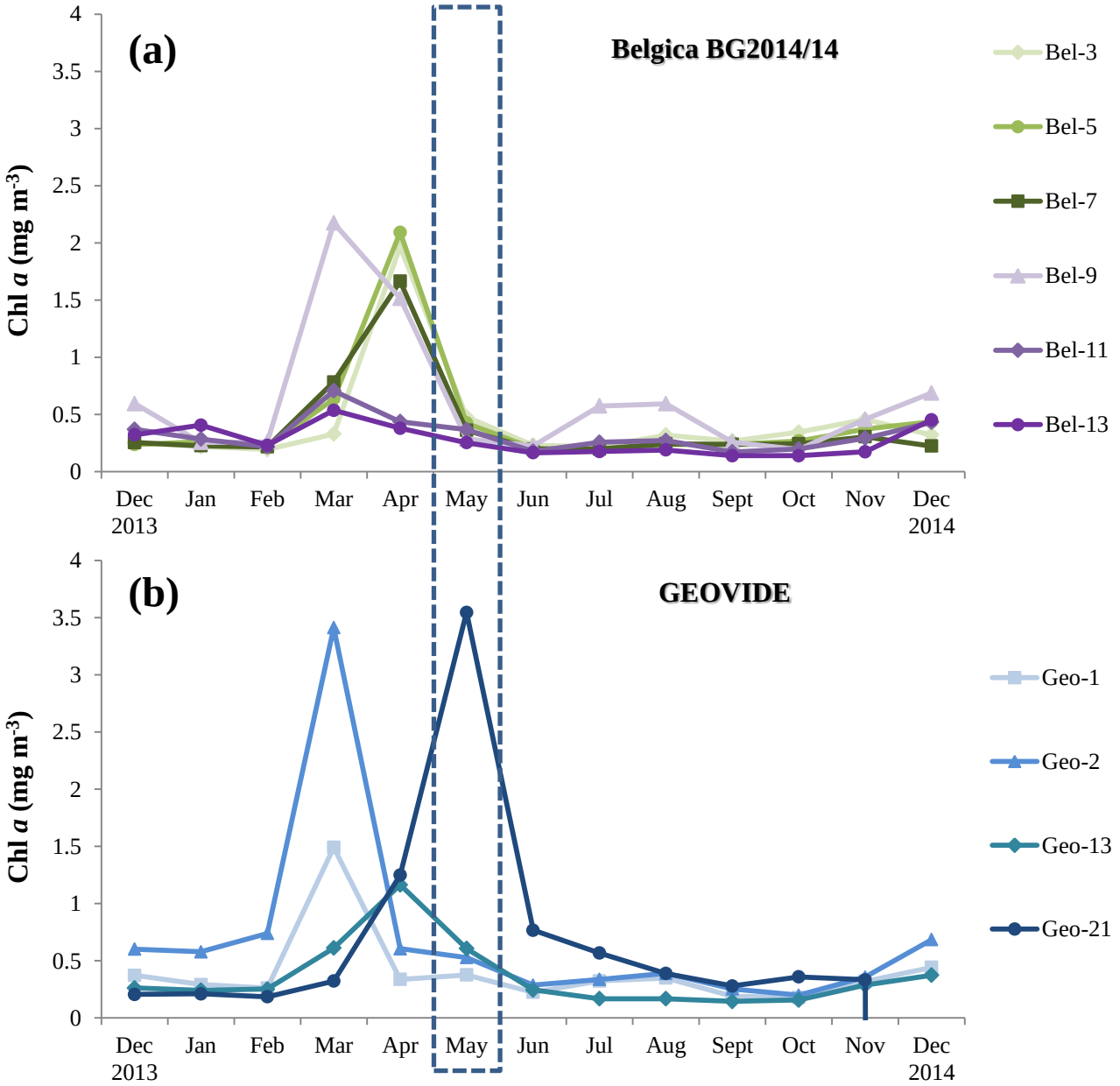
(a)
Belgica BG2014/14
Chl a (mg m-3)
4
3.5
3
2.5
2
1.5
1
0.5
0
Dec 2013
Jan
Feb
Mar
Apr
May
Jun
Jul
Aug
Sept
Oct
Nov
Dec 2014
Bel-3
Bel-5
Bel-7
Bel-9
Bel-11
Bel-13
(b)
GEOVIDE
Chl a (mg m-3)
Geo-1
Geo-2
Geo-13
Geo-21

Figure 4

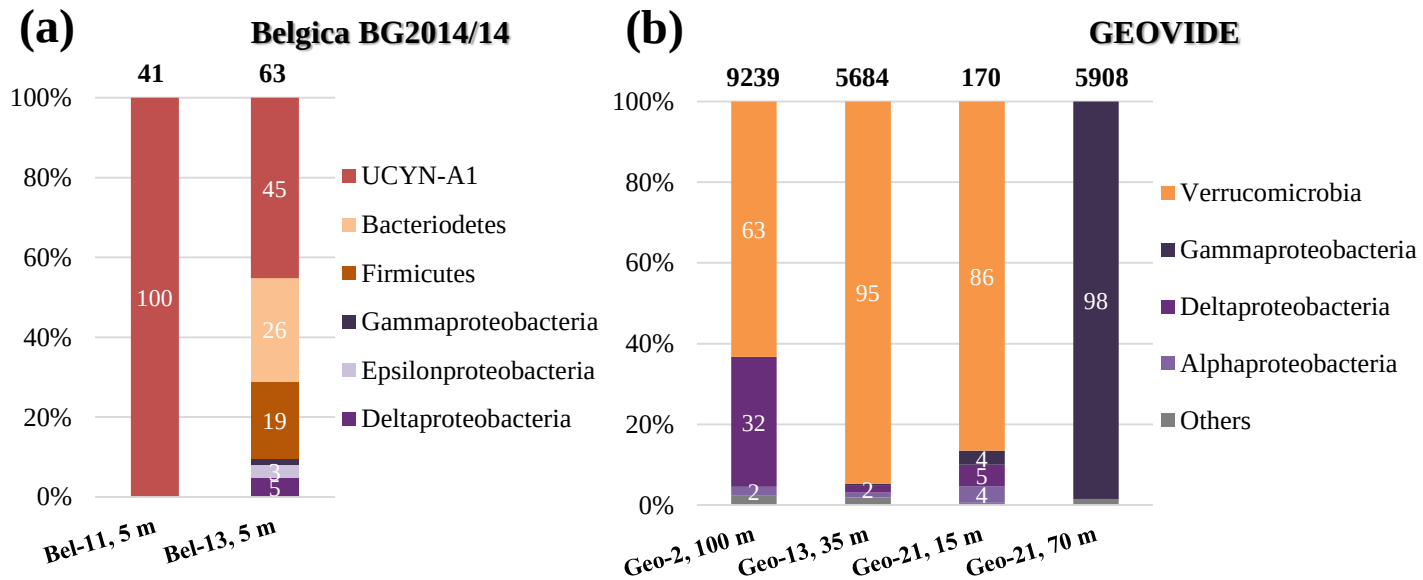
(a)
Belgica BG2014/14
41
63
100%
80%
60%
40%
20%
0%
100
45
26
19
3
5
UCYN-A1
Bacteriodetes
Firmicutes
Gammaproteobacteria
Epsilonproteobacteria
Deltaproteobacteria
Bel-11, 5 m
Bel-13, 5 m
(b)
GEOVIDE
9239
5684
170
5908
100%
80%
60%
40%
20%
0%
63
32
2
95
2
86
4
5
4
98
Verrucomicrobia
Gammaproteobacteria
Deltaproteobacteria
Alphaproteobacteria
Others
Geo-2, 100 m
Geo-13, 35 m
Geo-21, 15 m
Geo-21, 70 m

Figure 5


Candidatus Atelocyanobacterium thalassa isolate SIO64986
KY579326.1 - Bel-13 OTU1
KY579322.1 - Bel-11 Bel-13 OTU1
cyanobacterium endosymbiont of Epithemia turgida
L15554.1 Gloeothece sp. PCC 6909
Crocosphaera watsonii WH 8501
Cyanothece sp PCC 8801
Cyanothece sp PCC 7425
L15550.1 Lyngbya lagerheimii UTEX 1930
Nostoc punctiforme PCC 73102
Anabaena variabilis ATCC 29413
Nostoc sp. PCC 7120
Trichodesmium erythraeum IMS101
Denitrovibrio acetiphilus DSM 12809
Sulfuricurvum kujiense DSM 16994
Arcobacter nitrofigilis DSM 7299
Sulfurospirillum barnesii SES-3
KY579323.1 - Bel-13 OTU2
Sulfurospirillum cavolei
Teredinibacter turnerae T7901
MH974787 - Geo-21 NR237
MH974794 - Geo-2 Geo-13 Geo-21 NR
MH974782 - Geo-2 Geo-13 Geo-21 BB40
TARA ANW MAG 00019
TARA PSW ANW MAG 00006
TARA ION MAG 00014
TARA PON MAG 00023
TARA PSE MAG 00116
AF111110.2 Vibrio diazotrophicus
Methylomonas denitrificans
Shewanella sp. YQH10
Magnetococcus sp. MC-1
Erwinia carotovora subsp. atroseptica SCRI1043
KY579328.1 - Bel-13 OTU3
Dickeya dadantii 3937
Klebsiella michiganensis strain 628
Kosakonia sacchari SP1
Pantoea sp. At-9b plasmid pPAT9B03
CP002622
FN813564
Pseudomonas stutzeri A1501
FR669138.1 Pseudomonas stutzeri
Frankia sp. EAN1pec
MH974795 - Geo-2 Geo-13 Geo-21 NR0
Rhizobium leguminosarum bv. viciae 3841
Rhodomicrobium vannielii ATCC 17100
X51500.1 Azospirillum brasilense NifH gene
Novosphingobium malaysiense MUSC 273
Novosphingobium sp. MBES04
AF378718
Methylocella silvestris BL2
Burkholderia vietnamiensis strain G4
Leptothrix cholodni SP-6
Desulfuromonas acetoxidans DSM 684
Geobacter metallireducens GS-15
Pelobacter carbinolicus DSM 2380
MH974784 - Geo-13 NR498
Pelobacter seleniigenes DSM 18267
Paludibacter propionicigenes WB4
Brenneria goodwinii strain FRB141
KY579325.1 - Bel-13 OTU8
Candidatus Adiutrix intracellularis isolate Adiu1
Desulfovibrio legallii strain KHC7
Clostridium acetobutylicum ATCC 824
Clostridium pasteurianum strain M150B
Parasporobacterium paucivorans DSM 15970
KY579337.1 - Bel-13 OTU5
Clostridium aerotolerans DSM 5434 A
Clostridium sp. 12(A)
KY579332.1 - Bel-13 OTU4
KY579329.1 - Bel-13 OTU6
KY579327.1 - Bel-13 OTU13
KY579330.1 - Bel-13 OTU11
KY579335.1 - Bel-13 OTU14
Bacteroides graminisolvens DSM 19988 JCM 15093
KY579336.1 - Bel-13 OTU12
Dysgonomonas gadei ATCC BAA-286 cont1.10
KY579334.1 - Bel-13 OTU9
Bacteroides luti strain DSM 26991
Chlorobium phaeobacteroides BS1
Desulfovibrio bastinii DSM 16055
MH974783 - Geo-2 NR47
Desulfovibrionales bacterium GWA2
KY579331.1 - Bel-13 OTU7
Opitutaceae bacterium TAV5
MH974785 - Geo-2 Geo-13 Geo-21 NR176
MH974791 - Geo-2 Geo-13 NR84
MH974792 - Geo-2 Geo-13 Geo-21 NR2
Coprococcus catus GD/7 draft genome
Ruminococcus sp. SR1/5 draft genome
KY579324.1 - Bel-13 OTU15
KY579333.1 - Bel-13 OTU10
AB019138.1 Methanobrevibacter smithii
Cluster I
Cluster II
Cluster III
Cluster IV
0.50

Figure 6

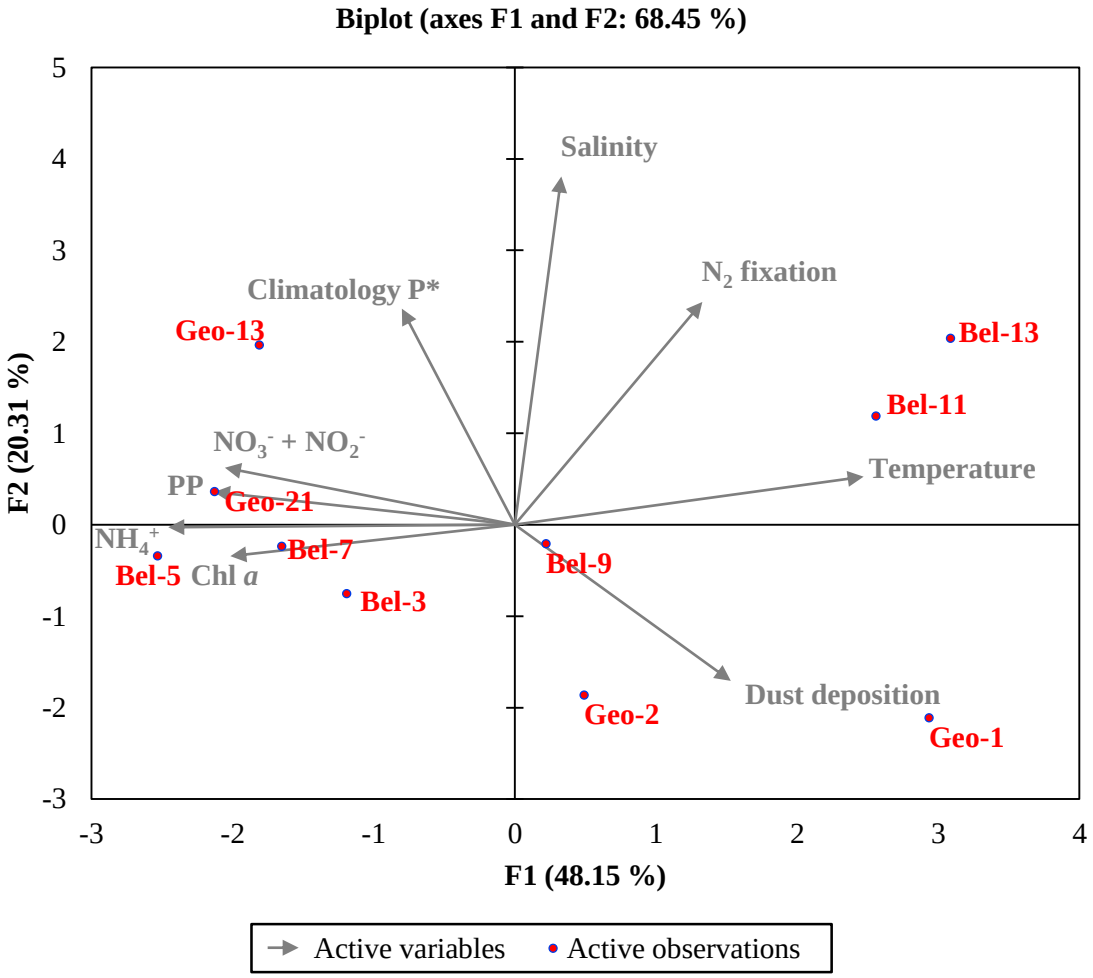
Biplot (axes F1 and F2: 68.45 %)
F2 (20.31 %)
F1 (48.15 %)
Salinity
N2 fixation
Climatology P*
Geo-13
Bel-13
Bel-11
NO3- + NO2-
Temperature
PP
Geo-21
NH4+
Bel-7
Bel-9
Bel-5
Chl a
Bel-3
Dust deposition
Geo-2
Geo-1
Active variables
Active observations

Figure 7